https://doi.org/10.5194/egusphere-2026-3638
Preprint. Discussion started: 8 July 2026

Development of a National-Scale Rip Current Forecast for Aotearoa New Zealand

Christopher Stokes[1], Juliana Albertoni de Miranda[2], Tim Scott[3], Gerd Masselink[3], Adam Wooler[4]

[1]Ocean Forecasting Research and Development, Met Office, Exeter, EX1 3PB, United Kingdom
[2]Surf Life Saving New Zealand, Lower Hutt (Wellington), 5010, New Zealand
[3]School of Biological and Marine Sciences, University of Plymouth, Plymouth, PL4 8AA, United Kingdom
[4]Beach Safety Consultants, Minstead, SO43 7FP, United Kingdom

Correspondence to: Christopher Stokes (christopher.stokes@metoffice.gov.uk)

Abstract. Rip currents are dangerous flows in the surfzone of wave-exposed coasts and can take bathers from the shallows into deeper water. They cause hundreds of drownings globally each year and are the leading cause of all beach lifeguard rescues. In New Zealand, with a population of approx. 5 million people, rip currents typically cause 500-1000 lifeguard rescues each year and are attributed to 53% of all Surf Life Saving New Zealand rescues. This study aims to identify environmental conditions associated with rip current incidents and develop a simple algorithm for forecasting rip current risk and hazard. A dataset of ~9,000 recorded rip current rescues along with water user head counts made at 58 beaches by lifeguards around the coast of New Zealand between 2001 and 2022 was used to assess rip current risk (parameterised from the total number of incidents) and rip current hazard (parameterised as the likelihood of an individual being in a rip incident) under different wave, tide, and wind conditions. In concurrence with previous findings, most rip incidents in New Zealand were recorded at beaches with intermediate 'bar-rip' beach morphology and occurred disproportionately during wave conditions at or above average breaker height with tide level at or below average low tide. Although rip incidents were also recorded at dissipative and reflective beaches lacking in bar-rip morphology, water users were 4 and 24 times more likely, respectively, to be in a rip-related incident at intermediate beaches with bar-rip morphology. A simple, threshold-based algorithm was developed using only breaker height, relative tide level, and a binary bar-rip morphology variable as predictors for use as a national-scale rip forecast across New Zealand. The algorithm achieves a high incident hit rate, capturing 98% of historic rip incidents across New Zealand, and captures exponentially increasing hazard at each of its five Rip Index levels, with a water user 6 times more likely to be in a rip incident at the highest Rip Index (~1-in-200) compared to the lowest (~1-in-1200). It also conservatively replicates a lifeguard's perception of rip hazard, with an overall agreement rate of approximately 81%, indicating it could provide useful forewarnings to the public especially at non-lifeguarded beaches or outside lifeguard patrol hours. To our knowledge, this represents the longest running rip incident data set analysed, and most widely validated rip forecast in the literature to date.

https://doi.org/10.5194/egusphere-2026-3638
Preprint. Discussion started: 8 July 2026

1 Introduction

Along the world's wave-dominated coasts, rip currents or 'rips' cause hundreds of drownings and tens of thousands of rescues globally each year and are the leading cause of all beach lifeguard rescues, including those made in New Zealand where the present study is focussed (Brighton et al., 2013; Castelle et al., 2016). A rip current occurs when wave breaking in the surfzone creates a reduction in momentum flux, resulting in wave induced set up at the shore (Longuet-Higgins and Stewart, 1964). Gradients in the set up drive flows alongshore which return back out to sea in concentrated and often fast-moving, O(0.5-1 m s^{-1}), offshore flows (Brander, 1999; MacMahan et al., 2006). These surfzone currents can carry water users from the shallows out into deeper water where panic, exhaustion, and in some cases drowning, can occur (Brander et al., 2011; Cornell et al., 2023).

Increasing rip current flow speed and decreasing surfzone retention increase bathing hazard by increasing the difficulty with which a bather can return to shore (Austin et al., 2013; McCarroll et al., 2014, 2015; Scott et al., 2014). Field experiments and numerical simulations have shown that rip current velocity increases with wave height and period (Castelle et al., 2006, 2020; MacMahan et al., 2005, 2006), as well as shore-normal wave incidence in the case of channel rips (Castelle et al., 2020; Long and Özkan-Haller, 2016; Moulton et al., 2017). However, there is some ambiguity regarding whether larger waves always induce a higher level of rip current hazard. Larger waves breaking further from shore saturate the surfzone inducing cellular circulation, limiting flow velocities within channels (Castelle et al., 2014), and reducing the proportion of surfzone exits (MacMahan et al., 2010). Scott et al. (2014) proposed that wave power at or just below the seasonal mean provides optimised breaking over the template morphology, inducing the strongest rip flows and highest proportion of surf zone exits. They found this correlated with the highest occurrence of rip incidents and periods of high rip hazard, defined using rip incident totals normalized by surf zone population (Eq. (1)), in the UK over the 5-year period they studied. On the other hand, Castelle et al. (2020) found that wave power at or in excess of the mean was associated with the highest prevalence of fatal and non-fatal rip-related drownings in France.

Bathymetrically-controlled rip currents ("channel rips" and "focused rips") are the most studied and well understood rip current type (Brander and Scott, 2018) and are synonymous with intermediate morphological beach states (Wright and Short, 1984), where alongshore variable wave breaking caused by subtidal sandbars is the primary driver for rip currents. Bathymetrically-controlled rips are sensitive to water level, with low tide levels enhancing wave focussing and breaking over surfzone sandbars as well as reducing the cross-sectional area of, and enhancing flow velocity through, intervening rip channels (Aagaard et al., 1997; Austin et al., 2010, 2014; Brander, 1999; MacMahan et al., 2005; Sonu, 1972). As a result, low tide levels have been widely linked to increased occurrence of rip incidents (Castelle et al., 2020; Engle et al., 2002; Scott et al., 2014) and rip related drownings (Arun Kumar and Prasad, 2014; Castelle et al., 2020), even in microtidal settings such as Australia (Koon et al., 2023). Rip currents are less commonly observed on non-intermediate beach types, but hydrodynamic instabilities in the surfzone ("shear instability rips" and "flash rips"), and control of wave-driven flows by headlands or other boundaries

https://doi.org/10.5194/egusphere-2026-3638
Preprint. Discussion started: 8 July 2026

("deflection rips", "shadow rips", and "cellular circulation") can cause rips to occur at non-intermediate beaches or on planar portions (for example, upper intertidal) of intermediate beaches (Castelle et al., 2016; Scott et al., 2012).

Rip current forecasts have been developed in previous studies dating back to the 1990s, with the aim of forewarning members of the public or informing lifeguarding operations. These early forecasts developed rip hazard indexes for the eastern coast of the USA, linking rip occurrence initially to strong winds (Lushine, 1991) and later to the presence of long-period swell waves (Lascody, 1998), wave direction, and tide (Engle et al., 2002). Dusek and Seim (2013) provided a significant contribution to these efforts, developing a probabilistic rip forecast using lifeguard rip intensity estimates made over two summers, and further validating against 741 lifeguard rescues made over nine summers, at one beach in North Carolina. They linked (in order of decreasing predictive power) significant wave height, wave direction, tide level, and a 'post-wave event' parameter, intended to represent periods of increased morphological relief, to binary 'rip or no-rip' lifeguard observations. One of the first nationally-operational rip forecasts (2014-present) was developed in the UK, based on in-situ rip measurements (Austin et al., 2014; Scott et al., 2014) and numerical modelling (Austin et al., 2013) at Perranporth Beach, UK, as well as rip incident statistics (n = 6,458) collected at 20 bar-rip beaches in southwest UK over 5 summer seasons (Scott et al., 2014). The system predicts 5 different Rip Index levels based on thresholds of wave power relative to the seasonal mean (parameterised as $Wfac$, Eq. (2)), daily low tide level relative to mean low water (parameterised as $Tfac_{LW}$, Eq. (3)), a binary bar-rip beach morphology variable, and wind speed (Scott et al., 2022).

Examples of other operational rip forecasts include a system developed from rip drowning statistics collected across India (n = 388) over 11 years (Arun Kumar and Prasad, 2014), a system for four beaches in Korea developed from physics-based modelling of flow velocities at Hyundai Beach (Lee et al., 2018), and a combined rip and estuary current forecast developed from physics-based modelling at Crantock beach in England (Stokes et al., 2024). Recently, simplified physics-based rip forecasts are starting to be developed (Casper et al., 2024; Castelle et al., 2024) which overcome some of the computational expense that has prohibited the widescale use of process-based models in operational rip forecasts. These show promising skill when tested against lifeguard recorded hazard perceptions and rip incident records but are so far limited in application to channel rips and have only been calibrated and tested at individual beaches.

The present study aims to assist in the management and mitigation of rip current hazard in New Zealand by developing a simple predictive algorithm that can be operationalised within a national-scale rip current forecast system. The objectives of the research are to:

1. Identify environmental conditions associated with high rip current hazard in New Zealand
2. Develop a simple algorithm that is effective at predicting the occurrence of rip current incidents and that can differentiate times of low and high hazard
3. Assess the performance of the rip prediction algorithm by comparing its predictions to historic rip incidents and lifeguard perceived rip hazard

https://doi.org/10.5194/egusphere-2026-3638
Preprint. Discussion started: 8 July 2026

2 Methodology

This study uses a large number of lifeguard-recorded, rip-related bathing incidents and links these to hindcasted wave, tide, and wind conditions to develop a predictive algorithm. When using this approach, it is important to account for both the number of water users present at a given time and the background distribution of each met-ocean forcing parameter, otherwise the system could unintentionally predict rips during the most popular or most frequently occurring marine conditions, rather than the most hazardous. A threshold-based algorithm is developed in Sect. 0 to predict rip current hazard by identifying conditions associated with disproportionately high (i.e. outside the background distribution) occurrences of rip incidents. To account for water-user exposure, the algorithm was validated for its ability to differentiate times of low and high rip hazard, parameterised as the likelihood of an individual being involved in a rip incident. The predictions of rip hazard were then compared to lifeguard perceptions of rip hazard at different times and locations around New Zealand.

2.1 Study setting

New Zealand's coasts (Fig. 1) are exposed to waves from the Pacific Ocean to the north and east, the Tasman Sea to the west, and the Southern Ocean to the south. The west and south facing coasts of New Zealand have an extremely energetic wave climate resulting from eastward propagating low pressure systems within the mid-latitude storm track. As a result, these coasts experience powerful breakers from locally generated storm waves and swells propagating from the Southern Ocean, with mean and maximum significant wave heights at the coast of 3 m and 10 m, respectively, and mean zero-crossing period of 8 s (Albuquerque et al., 2021; Gorman et al., 2003). The east facing coastline is largely sheltered against the dominant south-westerly wave approach but still receives locally generated storm waves and south-westerly swells that propagate around the land mass to the east facing beaches (Coggins et al., 2016), resulting in mean and maximum significant wave heights at the coast of 2 m and 9 m, respectively, and mean zero-crossing period of 7 s (Albuquerque et al., 2021; Gorman et al., 2003). The north-east facing coastline is the most sheltered overall, with mean and maximum significant wave heights at the coast of 1 m and 8 m, respectively, and mean zero-crossing period of 6 s (Albuquerque et al., 2021; Gorman et al., 2003).

New Zealand has mixed semi-diurnal tides, predominantly in the meso-tidal (2-4) range with some microtidal (< 2 m range) locations. The largest and smallest tides occur on the west and east coasts, respectively, at opposing sides of the Cook Strait (Costa et al., 2023), which divides the north and south islands. Due to a complete 360° range of tidal phases, there is both a high and low tide occurring along the New Zealand coast at any given time (Walters et al., 2001). The varied tide, wave, and sediment characteristics result in a wide range of coastal morphotypes (Hesp et al., 1999), including all major beach morphology states (Wright and Short, 1984) except those limited to macro-tidal environments.

New Zealand's beaches are popular with locals and tourists due to their picturesque nature and amenity value for leisure and water-sports activities, such as surfing and swimming. Surf Life Saving New Zealand (SLSNZ) is the primary beach and coastal safety, drowning prevention and rescue authority and provides beach lifeguard services at 92 locations during the summer season (Fig. 1, main panel), utilising >4,500 volunteer surf lifeguards. Through their lifeguard and emergency

https://doi.org/10.5194/egusphere-2026-3638
Preprint. Discussion started: 8 July 2026

response services, SLSNZ collects Incident Report Forms and water user head counts in their daily logs that provide an extensive catalogue of surfzone incidents back to the start of the 21st century.

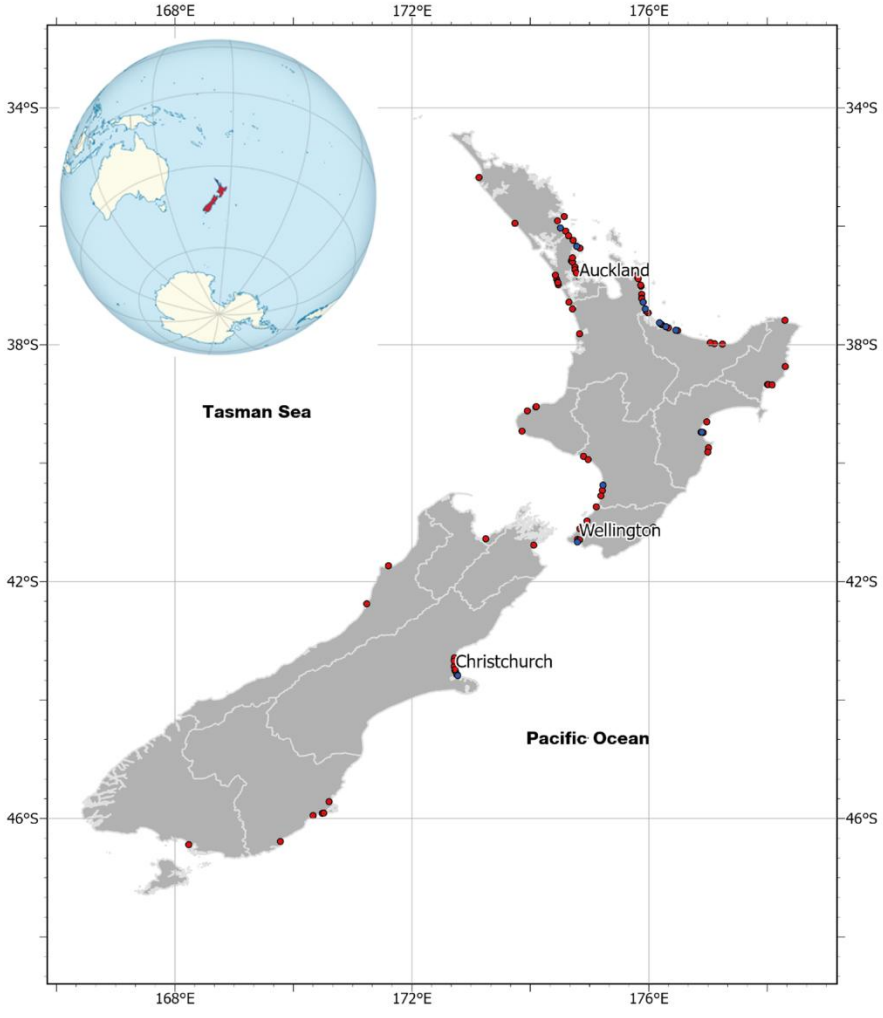

Figure 1.Sitemap of New Zealand highlighted in red in the inset map showing global position surrounded by the Pacific Ocean (to the east), Tasman Sea (to the west), and Southern Ocean (to the south). The main map shows North Island and South Island with locations of the 92 SLSNZ lifeguard patrolled beaches as circles. Blue circles show the location of the 12 SLSNZ beaches where lifeguard perceptions of rip current hazard were gathered for this study.

https://doi.org/10.5194/egusphere-2026-3638
Preprint. Discussion started: 8 July 2026

2.2 Incident and head count data

Lifeguard incident data enables identification of environmental conditions associated with rip current incidents and allows us to verify whether or not an algorithm would have correctly given a rip current warning at the time of a past incident. Including both rip and non-rip related incidents, between December 2001 and November 2022, a total of 49,881 Incident Report Forms were recorded across 92 SLSNZ patrolled beaches, involving 53,847 individuals and 21,090 lifeguard rescues. Key data variables for the present analysis are the time and location at which the incident took place, the number of people rescued, the estimated cause of the incident, and a classification of the severity of the incident ('Life Threatening', 'Involved Rescue', 'Involved First Aid', 'Involved Search', 'Near Miss', or 'Patient Assistance'). Lifeguard rescues of any severity which were attributed to rip currents were considered (n = 11,121), which removes non-rip related incidents and first aid incidents not requiring lifeguard in-water response. Herein, each reference to an incident represents one individual person being rescued from a rip current. 58 SLSNZ patrolled beaches had all the required met-ocean data for the present study and could therefore be included in the analysis, reducing the usable dataset of time-stamped incidents to n = 9,811 individual rip current rescues. This dataset was used to analyse environmental conditions associated with rip current incidents.

A further subset of 8,911 incidents was recorded at 58 beaches where head count data were also available, enabling the probability of an individual water user being involved in a rip current incident to also be computed at those beaches (Sect. 0). SLSNZ lifeguards routinely conducted hourly head counts of people in the water during patrol hours since approximately 2016 and recorded these in their daily logs. Before 2016, some clubs recorded estimates of the average head count across each day. In either case, the head counts represent an estimate of the number of people present in the water at a given point in time (instantaneous exposure), and do not represent the cumulative number of water users over the observation period. Although it is accepted that head count data are not always accurate, especially when large numbers (e.g., hundreds or even thousands) of water-users are present or where daily averages are provided, the head count estimates provide an approximate means by which to normalise the number of incidents occurring to account for the fact that more incidents are likely to occur when more people are present.

2.3 Exposure, life risk, and hazard

A key objective of this study is to predict when the physical hazard posed by rips is maximised. In the context of emergency and disaster risk management, the World Health Organisation (WHO) considers 'Life Risk' (number of life-threatening incidents) to be the product of 'Exposure', 'Hazard', and 'Vulnerability' (Kennedy et al., 2013; Saulnier et al., 2020). For example, a high degree of Life Risk could occur at a beach when only modest rip flows are present if the Exposure (number of water-users present) is sufficiently high or if those water users are particularly vulnerable to the hazards due to low water competency or hazard awareness. Conversely, low Life Risk might occur at a beach with highly hazardous rip current flows if few people enter the water, or if the water users have high surfzone competence.

https://doi.org/10.5194/egusphere-2026-3638
Preprint. Discussion started: 8 July 2026

With enough observations, this conceptual relationship allows us to parameterise rip current hazard P_{rip} using incident counts n_{inc} (Life Risk) and water user head counts n_{exp} (Exposure), as the probability of an individual water user requiring rescuing from a rip current over a given time period using the following form (Kennedy et al., 2013; Saulnier et al., 2020; Stokes et al., 2017):

$$P_{rip} = n_{inc}/n_{exp} \quad (1)$$

This parameterisation provides a proxy for the underlying physical hazard, estimated by normalising the number of incidents that occur by the number of water users exposed to the hazard. As water user vulnerability influences the number of incidents that occur, P_{rip} has to be averaged over many observations to provide useful quantification of the physical rip hazard for a given set of forcing conditions. Equation (1) then approximates the hazard level for a water user of 'average' vulnerability (swimming ability, water competency). P_{rip} was quantified for each beach by discretising the lifeguard data into two-hour time bins and dividing the number of incidents that occur in each time period by the instantaneous number of water users counted by the lifeguards. Only forcing combinations associated with at least 20 hours of lifeguard observations were used to estimate P_{rip}. A subset of 'high-hazard' events were also analysed, defined as conditions where P_{rip} exceeds the 90th%ile; equivalent to P_{rip} = 0.2, or 1 rip-related incident per 5 people in the water.

2.4 Wave, tide, and wind conditions

Wave, tide, and wind conditions were used in this study to investigate environmental conditions associated with rip incidents, and to generate hindcast rip hazard predictions. Wave conditions were obtained from a validated wave model hindcast with a 9 km spatial resolution (Albuquerque et al., 2021) which provided three-hourly time series of nearshore wave characteristics (significant wave height, Hs, peak wave period, Tp, and mean wave angle, Dm) for each SLSNZ beach over the study period. Local wind conditions (direction and magnitude) were estimated using the wave model forcing wind data. Time series of tidal water level were predicted for each site using a model developed by the National Institute of Water and Atmosphere (NIWA, https://tides.niwa.co.nz/). The hindcast wave conditions are well correlated with observed conditions (Pearson Correlation, R ≈ 0.9, 0.8 and 0.7 for Hs, mean period, and mean direction, respectively) and have Normalised Root Mean Squared Errors on the order of 10% for wave height and mean period (Albuquerque et al., 2021). Predicted tidal levels are expected to be accurate to within approximately +/- 20 cm, neglecting storm surge effects.

Breaking wave conditions are important to rip current analysis (Dusek and Seim, 2013) as wave refraction, shoaling, and sheltering in the nearshore alter surfzone wave power, breaker type, and momentum flux. For the present study, breaking significant wave height H_b was estimated from the wave model output depth (typically 10-30 m) using the formula of Larson et al. (2010), which computes incipient breaking wave conditions using a simplified wave energy flux conservation equation combined with Snell's law. This assumes shore-parallel depth contours and does not account for complex nearshore bathymetry such as reefs and sandbars or sheltering from small headlands not resolved by the wave hindcast model. Despite this

https://doi.org/10.5194/egusphere-2026-3638
Preprint. Discussion started: 8 July 2026

shortcoming, it provides a consistent method to estimate surfzone conditions on a national scale that would not be feasible using process-based modelling due to computational demand and lack of surfzone bathymetry data.

Wave, tide, and wind factors were also developed following the approach used in the UK's national-scale rip forecast (Scott et al., 2014, 2022). The dimensionless 'wave power factor' $Wfac$ represents the level of forecasted wave power relative to the average wave power at a given beach. $Wfac$ was computed from wave conditions shoaled to 10m depth $Wfac_{10m}$ and for breaking conditions $Wfac_b$:

$$Wfac = H_s T_p / \overline{H_s T_p} \quad (2)$$

where the overbar signifies time averaging across the austral summer months (DJF). We also test two forms of the tide factor, $Tfac$ (Eqs. 3 and 4). The first form ($Tfac_{LW}$) from Scott et al. (2014) represents the daily low tide level relative to average low tide at a given beach, with units of meters. Values below zero indicate larger than average (i.e. spring) tidal range on a given day. The second dimensionless form ($Tfac$) parameterises the instantaneous predicted tide level as a proportion of the average tide range for a given site, with values of 0 and 1 equal to average low and high tide levels, respectively:

$$Tfac_{LW} = LW - \overline{LW} \quad (3)$$

$$Tfac = (\eta - \overline{LW})/(\overline{HW} - \overline{LW}) \quad (4)$$

Here, η = water level, HW and LW are high-water and low-water elevation, respectively, and the overbars signify time averaging across the austral summer months (DJF). Normalised wind parameters were also computed, including the magnitude of the offshore directed wind component ('offshore wind'), where positive and negative values represent offshore and onshore directed wind velocity, respectively, and a 'wind factor' parameter which represents the absolute magnitude of the cross-shore directed wind component ($Wifac$).

2.5 Beach morphology classification

Each of the SLSNZ lifeguarded beaches was given a static beach morphology classification using a desk-study of satellite images. Typically, between 10-20 images spanning the years 2003-2023 were assessed for each beach, revealing visible bed features and surfzone breaker patterns (for example, Fig. 2) which were classified as either dissipative, intermediate (including longshore bar-trough, rhythmic bar and beach, transverse bar and rip, ridge runnel/low tide terrace), or reflective using the main beach classes from the Wright and Short (1984) beach state model. While it was beyond the scope of the present study to use information about beach slope or sediment size to inform the beach classification, the satellite images provide a view of the beach under a range of tide and wave conditions over multiple seasons and years and therefore allowed qualitative assessment of the dominant summer morphology type at each site.

https://doi.org/10.5194/egusphere-2026-3638
Preprint. Discussion started: 8 July 2026

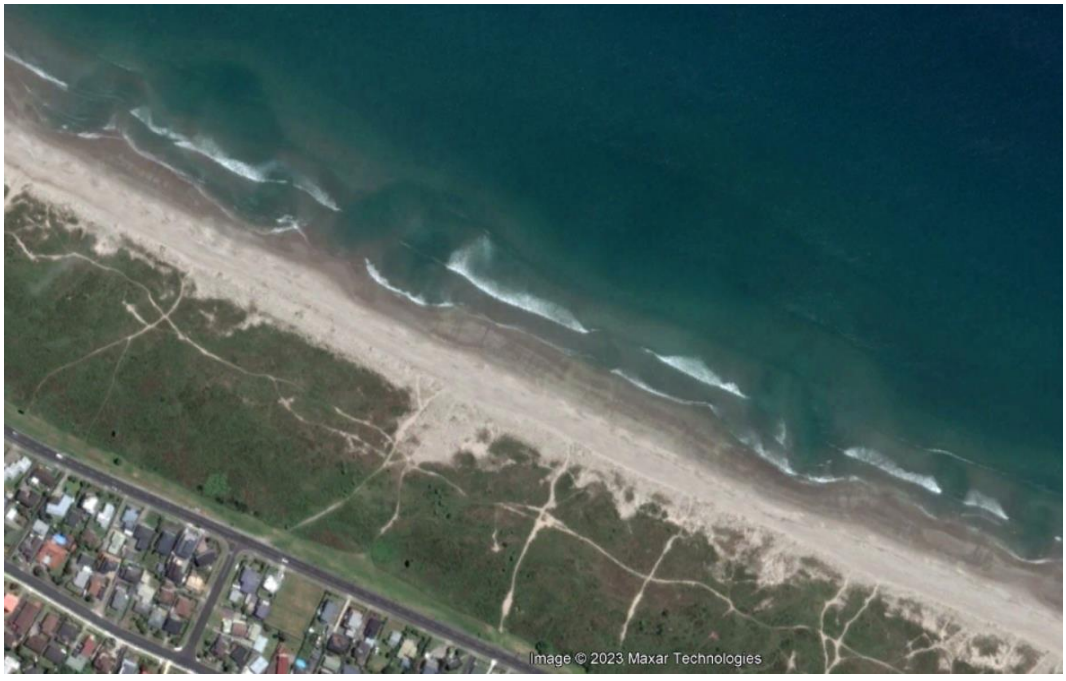

Figure 2. Example satellite image from Papamoa beach from November 2011 used to inform the beach morphology classification. In this example, 'transverse bar-rip' morphology features are visible from the subtidal beach surface and breaker patterns indicating an intermediate beach type.

2.6 Predictive skill and comparison to lifeguard perceived hazard

To assess the skill of the developed algorithm, we consider the proportion of observed incidents (n_{inc}) correctly associated with the upper Rip Index values (RI 2-5). This indicates a rip incident's 'probability of detection' by the algorithm (Panofsky and Brier, 1953), now more commonly referred to as the recall or rate of true positives achieved by the predictive system. We also examine how often the hindcast missed an incident (i.e. RI 1 was predicted when an incident was recorded), which represents the rate of false negatives. It was not possible to examine the rate of false positives because bathing hazard can be high without an incident occurring, for example if no one enters the water or due to lifeguard preventative actions. We test the system's ability to capture the 'observed' level of hazard by determining the average incident derived P_{rip} at each of the five Rip Index levels.

Another means to assess the effectiveness of a hazard warning system is to examine its efficiency. A system that gives warnings all the time will correctly predict all the risk and hazard but will be highly ineffective due to a high rate of false alarms and low levels of user confidence. Conversely, a system that gives out warnings sparingly but captures a disproportionate amount of risk and hazard with those warnings is likely to be effective as users are more likely to pay attention when warnings occur. Efficiency is quantified as the ratio of useful output to total input (Sickles and Zelenyuk, 2019) which in the present context can be represented as:

https://doi.org/10.5194/egusphere-2026-3638
Preprint. Discussion started: 8 July 2026

$$r = O/C \quad (5)$$

Where r is the efficiency of the rip hazard predictor, O is the proportion of incidents or high-hazard events captured (the 'useful output' of the system), and C is the proportion of time that warnings are given (the 'cost' of the system).

As a means to further verify the developed rip prediction algorithm, the predicted Rip Index levels were compared to lifeguard perceptions of rip hazard (Fig. 3), ranked on an equivalent 1-5 scale. The purpose of this assessment was to determine how well the predicted hazard replicates a lifeguard's perception of rip hazard. Over an austral summer season between September 2024 and February 2025, lifeguards at 12 beaches across New Zealand (Fig. 1) visually rated the rip hazard. The wave and tide conditions forecasted within 30 minutes of these observations were used to generate equivalent predictions of rip hazard from the developed algorithm. Lifeguards were provided with the rip index level descriptions in Table 1 as a reference. Lifeguards could rate the rip hazard any time during their patrols. The forecast used corresponded to the closest available forecast to the time the assessment was initiated. For example, if a lifeguard began an audit at 10:15 A.M., the forecasted values for 10:00 A.M. were used. Forecast data were available for each hour and refreshed every three hours, ensuring that the most recent information as close as possible to the time of the assessment was used. 10 of the 12 beaches were intermediate beaches featuring some form of bar-rip morphology, with 1 reflective and 1 dissipative beach also included in the observation exercise (Table A1).

https://doi.org/10.5194/egusphere-2026-3638
Preprint. Discussion started: 8 July 2026

Figure 3. Lifeguards observing surfzone conditions from the patrol tower at Papamoa Beach, North Island, New Zealand. Source: Surf Life Saving New Zealand.

3 Results

3.1 Comparison of rip incidents to environmental conditions

Rip currents were attributed to 53% of all SLSNZ recorded rescues over the study period. However, inconsistency in the method of attribution of incidents to rip currents within the Incident Report Forms (tick box versus free text entry) over certain time periods means that variation is seen in the proportion of incidents attributed to rip currents in some years (Fig. B1), and the true proportion may be higher. Similarly, police and coroner's reports have attributed rip currents to 17% of drowning deaths at surf beaches in New Zealand between January 2014 and June 2024 (Water Safety New Zealand, 2024), but this is expected to be an underestimate due to the challenges of attribution with substantive evidence often days after the drowning has occurred.

Fig. 4 shows that the majority of lifeguard data in New Zealand comes from intermediate (bar-rip) beaches, where 86% of all lifeguard patrol hours are undertaken. Furthermore, 96% of rip current rescues and 95% of the highest-hazard events (P_{rip} >

https://doi.org/10.5194/egusphere-2026-3638
Preprint. Discussion started: 8 July 2026

280 90th%ile) occurred at intermediate beaches. Dissipative and reflective beaches in comparison contribute far fewer rip incidents, at 3% and 1%, respectively. It is acknowledged that because the vast majority of lifeguards operate on intermediate beaches there is data imbalance between the three beach types (Fig. 4, left panel). This is symptomatic of the fact that rip currents most commonly occur on intermediate morphology beaches and that surf lifesaving clubs have often been formed on beaches where people have drowned or because those beaches were risk assessed by SLSNZ and found to require lifeguards, indicating a high
285 level of historical risk.

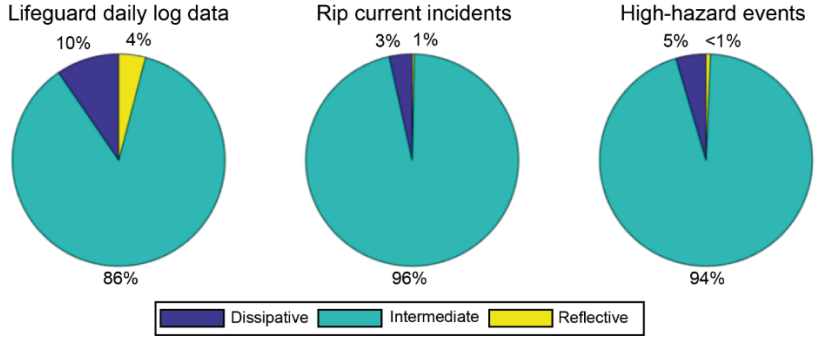

Figure 4. Proportion of observation effort (from number of lifeguard daily log entries), rip current incidents, and high-hazard events at the three main beach morphology types (dissipative, intermediate, reflective) from SLSNZ lifeguard data between 2001-2022,
290 **inclusive.**

Figure 5 compares normalised frequency distributions of the tested met-ocean parameters against distributions of conditions at the time of rip incidents. Rip incidents were recorded over almost the full distribution of each environmental variable, suggesting that rip hazard is present over a wide range of met-ocean conditions. The difference between the background and
295 incident related distributions is shown as either a positive or negative orange bar, with positive (negative) bars indicating conditions associated with disproportionately more (less) rip current incidents. Figure 5 (left panels) shows that rip incidents across New Zealand occurred disproportionately under moderately energetic wave conditions ($H_b \geq 1$ m, peak wave period $T_p \geq 8$ s, $Wfac \geq 1$), with tide level around average low tide level ($Tfac < 0.3$). Tide range also seems to have some importance, with rip incidents disproportionately more common during spring tides ($Tfac_{LW} < 0$; Fig. C1) than during neap tides. Low
300 wind speeds (Ws <5 m/s) also appear to be linked with a disproportionate increase in rip current incidents, relative to the occurrence of such winds.

These relationships also hold true for the most hazardous conditions observed ($P_{rip} > 90^{th}$%ile), as demonstrated in Fig. 5 (right panels), albeit with slightly elevated thresholds for breaker height ($H_b > 1.2$ m) and wave factor ($Wfac > 1.4$). Under increasingly large breaker heights the distribution of rip incidents is approximately the same as the background forcing
305 distribution, but some increase in high-hazard events is noticeable at $H_b > 2.5$ m (Fig. 5, top right panel). This confirms that the previously identified thresholds do not just relate to increased numbers of incidents (which could occur during the most popular conditions, for example), but that a higher level of overall hazard occurs during the identified conditions as well.

https://doi.org/10.5194/egusphere-2026-3638
Preprint. Discussion started: 8 July 2026

In general, the comparison between rip incidents and environmental forcing conditions suggests that there is a disproportionate increase in rip current $Risk$ and $Hazard$ when:

- $H_b \geq 1$ m
- $Wfac \geq 1$
- $Tfac < 0.3$
- Ws <5 m/s

Significantly fewer incidents were recorded at the 7 dissipative beaches studied (incidents = 327, high-hazard events = 16) and 2 reflective beaches studies (rip incidents = 28, high-hazard events = 2), than at the 49 intermediate beaches in the dataset (incidents = 9,456, high-hazard events = 430). The distributions are noisier at dissipative and reflective beaches due to the relatively low data counts. However, the thresholds remain relevant for each of the three main beach types studied (Appendix C). Across all the data, the average likelihood of a water user being involved in a rip incident $\overline{P_{rip}}$ at an SLSNZ lifeguarded beach is $\overline{P_{rip}}$ = 0.0020 (1 rip-related incident per 500 people in the water). However, this varies significantly between the main beach types, with hazard highest at intermediate beaches ($\overline{P_{rip}}$ = 0.0022) and significantly lower at reflective beaches ($\overline{P_{rip}}$ = 0.00009) and dissipative beaches ($\overline{P_{rip}}$ = 0.00062).

https://doi.org/10.5194/egusphere-2026-3638
Preprint. Discussion started: 8 July 2026

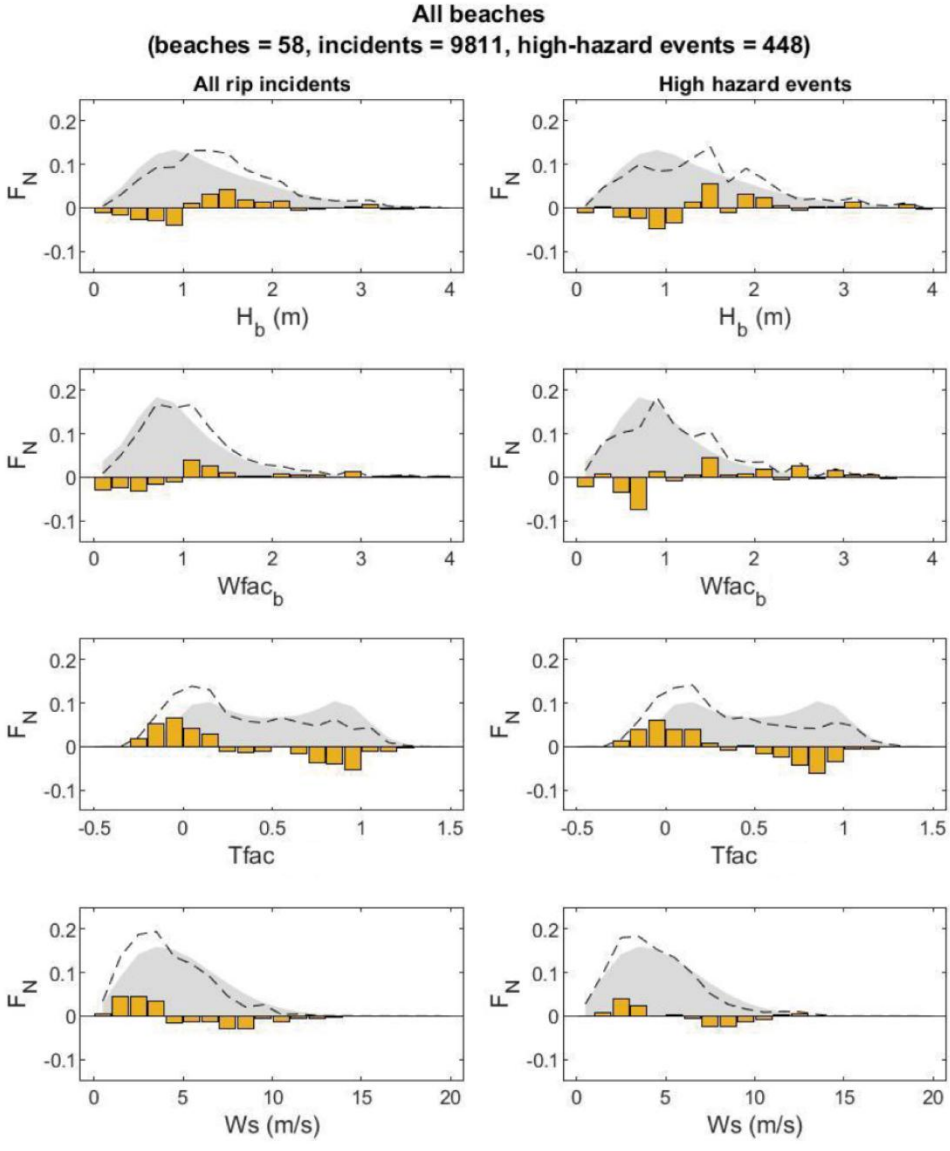

Figure 5. Normalised frequency distributions FN of key forcing variables at times of rip current incidents (left panels) and for P_{rip} > 90th%ile - 'high-hazard events' (right panels). From top to bottom panels show breaker significant wave height H_b, Wave Factor at break point $Wfac_b$, Tide Factor Tfac, and wind speed Ws. Dashed lines show conditions occurring during rip current incidents, while grey shaded areas show the background distribution that occurs naturally over the Austral summer (Dec, Jan, Feb). The difference between the background and incident related distributions is shown as either a positive or negative orange bar, with positive (negative) bars indicating conditions associated with disproportionately more (less) rip current incidents.

https://doi.org/10.5194/egusphere-2026-3638
Preprint. Discussion started: 8 July 2026

3.2 Rip forecast algorithm

To develop a predictive algorithm for rip current hazard, the transitions in forcing associated with a switch from disproportionately fewer to greater incident numbers (Sect. 0) were used as thresholds to define 5 'Rip Index' levels (Table 1). As H_b and $Tfac$ both displayed a strong relationship to rip incidents and high-hazard events, the algorithm relies on the identified thresholds in those parameters alongside a binary bar-rip beach morphology variable determined from an intermediate or non-intermediate morphology classification. Rip Index 1 is given during low energy wave conditions ($H_b \leq$ 0.5 m), when few incidents were recorded. Rip Index 2 is given under moderate waves (H_b≤1 m threshold) acting on non-bar-rip morphology, which is assumed to occur at any stage of the tide at non-intermediate beaches, or at intermediate beaches during mid to high tide levels ($Tfac$≥0.3 threshold). Rip Index 3 is given under either (a) energetic waves (H_b≥1 m threshold) at non-intermediate beaches, or (b) moderate waves (H_b≤1 m threshold) and low tide ($Tfac$≤0.3 threshold) at intermediate beaches. Rip Index 4 is only given under energetic waves when tide is at or below average low tide level at intermediate beaches (H_b≥1 m and $Tfac$≤0.3 thresholds). Rip Index 5 was included to capture high-energy conditions when surfzone currents (whether classically defined as rips or not) are likely to be strong (H_b>2.5 m threshold).

Using these thresholds a decision tree algorithm, herein referred to as the NZ Rip Forecast, was used to generate Rip Index predictions from predicted wave and tide conditions and the pre-determined beach morphology class. To assess the performance of the algorithm (Sect. 0), hindcast Rip Index predictions were generated over the time period 2001-2022 at an hourly resolution by applying the environmental forcing data described in Sect. 0 to the algorithm described in Table 1.

Table 1. Description of Rip Index levels and forcing thresholds used in the New Zealand Rip Forecast algorithm.

Rip Warning Level	Beach type	Forcing description	Thresholds	Physical driver
Rip Index 1: Low rip hazard	Bar-rip and non-bar-rip	Small waves (breaking waves < 0.5 m)	$H_b \leq 0.5$ m	Low wave energy
Rip Index 2: Moderate rip hazard	Bar-rip	Moderate waves (breaking waves between 0.5 and 1 m) and near high tide	0.5 m < $H_b \leq 1$ m $Tfac \geq 0.3$	Moderate energy waves acting on planar morphology
	Non-bar-rip	Moderate waves (breaking waves between 0.5 and 1 m)	0.5 m < $H_b \leq 1$ m	
Rip Index 3: High rip hazard	Bar-rip	Moderate waves (breaking waves between 0.5 and 1 m) and near low tide	0.5 m < $H_b \leq 1$ m $Tfac < 0.3$	Moderate energy waves acting on bar-rip morphology

https://doi.org/10.5194/egusphere-2026-3638
Preprint. Discussion started: 8 July 2026

	Non-bar-rip	Energetic waves (breaking waves between 1 and 2.5 m)	1 m < H_b ≤ 2.5 m	Energetic waves acting on planar morphology
Rip Index 4: Very high rip hazard	Bar-rip	Energetic waves (breaking waves between 1 and 2.5 m) and near low tide	1 m < H_b ≤ 2.5 m $Tfac$ < 0.3	Energetic waves acting on bar-rip morphology
Rip Index 5: Very high hazard	Bar-rip and non-bar-rip	High energy waves, strong currents (breaking waves > 2.5 m)	H_b > 2.5 m	High energy waves, strong currents

3.3 Performance of the Rip Forecast algorithm

3.3.1 Predicting rip current risk

Firstly, we compare hazard predications (RI 2-5) with incident occurrence (observed risk). Across the studied beaches, the recall (proportion of true positives) of the NZ Rip Forecast was 98% (Fig. 6). False negatives therefore occurred 2% of the time, with the algorithm predicting RI 1 (predicted $H_b \leq 0.5$ m) during those recorded incidents. This recall rate was achieved by issuing rip warnings (RI 2-5) 92% of the time; the low energy wave conditions associated with RI 1 therefore occurred a small proportion (8%) of the time at the studied SLSNZ beaches, but rip incidents also occurred infrequently (2%) under those conditions. Most past incidents occurred at RI 3 (39%) and RI 4 (42%). 10% of past rip incidents occurred when RI 5 was predicted by the algorithm. While RI 5 is intended to represent 'very high hazard', it is included in the forecasts to capture times when high wave energy drives very strong surfzone currents, regardless of whether they typify a rip current flow. Because RI 5 occurs only under very large waves when water-user exposure is expected to be reduced, the rip current risk is lower under RI 5 than at RI 4.

The efficiency of the algorithm (Eq. (5)) at predicting incidents increases as the RI level increases (Table 2). For example, looking at all warnings in excess of RI 1 the efficiency is just over 1, meaning that a slightly larger proportion of incidents happen at RI 2-5 than the proportion of time those warnings are given. However, for RI > 2 efficiency increases to 1.23, and at RI > 3 efficiency is 1.63. This suggests that warnings above those thresholds are given sparingly relative to the proportion of incidents they capture. For example, RI 4 was predicted 20% of the time but captured 42% of all SLSNZ rip incidents.

3.3.2 Predicting rip current hazard

The average rip current hazard occurring at each RI level was computed from the lifeguard incident and head count data using Eq. (1). Figure 6 indicates that the probability of a water user being involved in a rip incident increases exponentially from RI

https://doi.org/10.5194/egusphere-2026-3638
Preprint. Discussion started: 8 July 2026

1-5, with P_{rip} increasing an order of magnitude between RI 1 (P_{rip} = 0.0008) and RI 4 (P_{rip} = 0.0055) and remaining high at RI 5 (P_{rip} = 0.0048). 90% of the high-hazard events (P_{rip} > 90th%ile) occurred at RI 3-5. The algorithm captured slightly lower hazard at RI 5 than at RI 4, indicating that larger waves (RI 5) do not necessarily lead to higher hazard levels than moderate waves acting on low tide bar-rip morphology (RI 4).

As with rip current risk, the algorithm is increasingly efficient at capturing high-hazard events as RI increases (Table 2). For warnings above RI 1, the algorithm captures a slightly larger proportion of high-hazard events than the proportion of time warnings are given. The efficiency increases to 1.22 at RI > 2 and to 1.66 at RI > 3. This means that high-hazard events occur frequently at RI 3-5 relative to the number of warnings given.

For each of the three main beach morphology types (Dissipative, Intermediate, Reflective), increasing rip hazard was captured at RI 1-3 by the algorithm (Fig. 7). For non-bar-rip morphology (Dissipative and Reflective) beaches, an approximately linear increase in rip hazard is observed with increasing breaker height between RI 1-3, with Dissipative beaches exhibiting more rip current hazard at each RI level than Reflective beaches. The highest hazard levels and steepest increase in hazard with RI level occurs at bar-rip (intermediate) beaches, where an exponential increase in hazard was captured between RI 1-4 (Fig. 7). RI 4 only applies to bar-rip beaches and is a key level in the algorithm as it represents a high-risk, high-hazard scenario, when channel rip activity is expected to be at its peak. A slight decrease in hazard occurs at RI 5 for intermediate beaches. Few incidents occurred under RI 5 at dissipative beaches and no incidents at all occurred at RI 5 at reflective beaches.

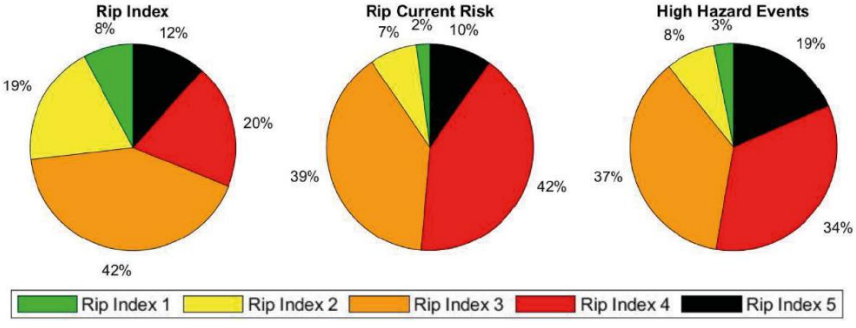

Figure 6. Summary of the performance of the NZ Rip Forecast against 22 years of SLSNZ rip incident data collected at 58 beaches (8,911 incidents). Proportion of Rip Index levels forecasted (upper left), proportion of rip current incidents 'Risk' at each Rip Index (upper right), average probability of an individual water user being involved in a rip incident 'Hazard' at each Rip Index (lower left), and proportion of high-hazard (P_{rip} > 90%ile) events at each Rip Index (lower right).

https://doi.org/10.5194/egusphere-2026-3638
Preprint. Discussion started: 8 July 2026

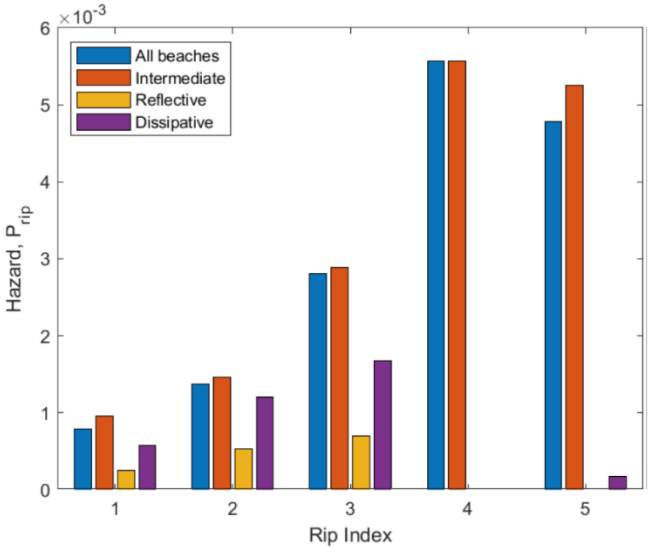

Figure 7. Average probability of an individual water user being involved in a rip incident, Prip, at each Rip Index level for different beach morphology types.

395

Table 2. Efficiency of the rip forecast algorithm at different Rip Index (RI) levels at capturing SLSNZ rip incidents (Risk) and proportion of high-hazard events. Values in excess of 1 indicate a disproportionate amount of rip risk and hazard is captured relative to how often that RI threshold is exceeded.

Rip Index level	Efficiency	
	Risk	High-hazard events
RI >1	1.06	1.05
RI >2	1.23	1.22
RI >3	1.63	1.66

400

3.3.3 Comparison to lifeguard hazard perceptions

Lifeguards conducted a total of 568 rip hazard assessments over the austral summer season between late September 2024 and
405 early February 2025 (Figure 8). Participation across the 12 patrol locations (Fig. 1) varied, with an average of 4.3 assessments per day. Perfect agreement between lifeguard observations and the forecast occurred in 53% of cases across all patrol locations.

https://doi.org/10.5194/egusphere-2026-3638
Preprint. Discussion started: 8 July 2026

When lifeguards perceived the hazard to be between RI 2 and RI 5 (i.e. when some level of rip hazard was present), the level of perfect agreement with the algorithm was between 64-86%. Among the 266 assessments where discrepancies were recorded, 158 ratings (28% of all assessments) were perceived to be one index level lower than the forecasted rip hazard.

There were few cases overall (1.58%) where the rip forecast algorithm underpredicted rip hazard relative to the lifeguard perceived hazard. However, 17% of the assessments rated at RI 4 or 5 by lifeguards were underestimated by 1-2 levels by the algorithm. Disagreements were most frequent when RI 1 was perceived by lifeguards. Under such conditions, the algorithm occasionally predicted up to RI 4, suggesting that the lifeguards perceived the hazard to be low despite the modelled wave conditions being $H_b \geq 1$ m in some cases.

Combining instances of perfect agreement with those perceived by lifeguards to be one RI level lower than the predicted RI provides a conservative measure of overall agreement. As such, it is reasonable to infer an overall agreement rate of approximately 81%. This indicates a generally high level of consistency between the rip forecast model and lifeguard perceptions of rip hazard, albeit with a tendency for the rip hazard algorithm to occasionally overpredict the lifeguard perceived hazard.

	Observation (%)					
Prediction (%)	**1 - Low Rip Hazard**	**2 - Moderate Rip Hazard**	**3 - High Rip Hazard**	**4 - Very High Rip Hazard**	**5 - Very High Hazard**	**All (count)**
1 - Low Rip Hazard	30	0	0	0	0	**81**
2 - Moderate Rip Hazard	38	66	0	0	0	**198**
3 - High Rip Hazard	27	25	85	18	14	**204**
4 - Very High Rip Hazard	5	9	14	64	0	**65**
5 - Very High Hazard	0	0	1	18	86	**20**
All (count)	**266**	**148**	**101**	**39**	**14**	**568**

Figure 8. Percentage of rip forecast predictions at each lifeguard perceived hazard level. Light to dark green indicates increasing levels of agreement. Totals (counts) are provided in the 'All' column and row.

4 Discussion

This study developed a threshold-based forecasting system for predicting times of high rip hazard using a large dataset of rip-related incidents and associated water user head counts. While a number of previous studies have developed rip forecasts with good predictive power, these have often been optimised and tested on relatively few years of data or using data from only one or a few beaches (Castelle et al., 2024; Dusek and Seim, 2013; Engle et al., 2002; Lee et al., 2018) and require further verification to determine how well the predictions generalise to other coastal settings. Prior to national implementation by the National Oceanic and Atmospheric Administration in the USA, the algorithm of Dusek and Seim (2013) was tested against in-situ flow measurements near Duck, North Carolina (Moulton et al., 2017) and additional lifeguard observations at five locations

https://doi.org/10.5194/egusphere-2026-3638
Preprint. Discussion started: 8 July 2026

across Florida, North Carolina, and California (Churma et al., 2017; Gibbs et al., 2015), indicating good correlation with rip intensity observations. That algorithm is already used to generate operational rip forecasts for New Zealand by the 'Swellmap' platform (https://www.swellmap.com/potential-rip-hazard-forecasts/new-zealand). However, the predictions may not represent rip hazard at beaches with significantly different wave climate, tides, and morphology to the 6 beaches on which it was developed, and consideration of many tens of sites in the optimisation and validation of a rip forecast is therefore desirable. Given the expense of fieldwork and numerical modelling, the use of incident data or lifeguard hazard perceptions are some of the only feasible means to achieve this. However, where larger scale studies of rip incidents have been undertaken, water-user numbers and forcing climatology have sometimes not been accounted for (Arun Kumar and Prasad, 2014), raising questions around whether physical hazard is being predicted or simply times when the most incidents occur. Such systems are susceptible to false negatives ('misses') as high hazard often occurs during inclement weather or large wave conditions when water user exposure, and therefore total incidents numbers are low (Castelle et al., 2020; Scott et al., 2014). The present study has sought to overcome these limitations by analysing ~9000 incidents collected at 58 beaches in New Zealand, accounting for water-user exposure and the background climatology of forcing variables.

The developed rip prediction algorithm is extremely simple and uses no statistical modelling other than the identification of thresholds in key forcing variables known to contribute to rip hazard. It uses just two temporally varying predictors (H_b and $Tfac$) and one 'static' binary predictor (intermediate beach type). The forcing thresholds, conceptual rip current behaviour, and hazard level associated with each Rip Index level are depicted in Fig. 9. These variable choices were informed by both the present analysis and by previous studies that have shown wave energy, tide, and beach morphology to be key factors driving rip hazard (Castelle et al., 2016). However, other predictor variables could have been included. The $Wfac$ parameter has been found in previous studies to correlate with occurrence of rip incidents (Castelle et al., 2019, 2024; Scott et al., 2014) and lifeguard hazard perceptions (Castelle et al., 2025). The present data set concurs with these previous findings, although contrary to Scott et al. (2014) we see disproportionately more rip incidents with $Wfac \geq 1$, supporting the observation of Castelle et al. (2020) that wave power in excess of the mean leads to the highest levels of rip current hazard. Similarly, rip incidents showed a clear increase when H_b exceeded 1 m in the present study - approximately the background mean value (Fig. 5). H_b was chosen to be included in the developed algorithm instead of $Wfac$ as it is a more intuitive parameter for non-scientists to understand, and because in highly sheltered (exposed) locations mean $Wfac$ is exceeded during very low (high) energy conditions which could lead to false positives (negatives).

Shore-normal wave incidence has been linked to increased rip flow speed in channel rips (Castelle et al., 2020; Dusek and Seim, 2013; Long and Özkan-Haller, 2016; Moulton et al., 2017), while oblique wave incidence is known to be important for boundary rip circulation (Mouragues et al., 2021; Scott et al., 2012). The importance of wave period on rip hazard has also been debated in the literature (Castelle et al., 2025; Moulton et al., 2017). Despite the lack of wave angle or period as predictors in the developed NZ rip forecast, it successfully differentiates risk and hazard across the five Rip Index levels. This may be because both wave angle to the shore and wave period are considered in the calculation of H_b, making it a functional predictor of rip hazard. Local wind velocity has been used for rip forecasting in at least two previous studies (Lushine, 1991; Scott et

https://doi.org/10.5194/egusphere-2026-3638
Preprint. Discussion started: 8 July 2026

al., 2022), but has been disregarded by others (Castelle et al., 2024; Dusek and Seim, 2013). The data from New Zealand shows an apparent link between light (<3 m/s) onshore directed winds and increased rip incidents and high-hazard events (Fig. 5), which concurs with previous observations that more incidents occur during either light winds (Engle et al., 2002; Scott et al., 2022) or onshore winds (Gensini and Ashley, 2010; Lushine, 1991). For example, Gensini and Ashley (2010) found that onshore winds were associated with 70% of rip drownings in the USA. Future research should therefore seek to clarify whether there is a physical mechanism linking onshore directed wind and rip current hazard, or whether the apparent links are an artefact of wind climatology.

The algorithm captures past rip incidents best at beaches with intermediate bar-rip morphology (99% recall) using thresholds based on breaker height and tide level, but acceptable skill is also achieved at reflective beaches (80% recall) and dissipative beaches (82% recall) using thresholds based on breaker height alone. While the vast majority of incidents (96%) and high hazard events (95%) were recorded at Intermediate beaches, rip incidents were recorded at Dissipative (3%) and Reflective (1%) beaches too. Given the lack of defined bar-rip features at those beach types, it is assumed those incidents are caused by either hydrodynamic instabilities such as flash rips, or boundary rip currents (Fig. 9). The acceptable recall and ability of the forecast to capture increasing P_{rip} using thresholds in breaker height alone suggests it is a useful indicator of rip hazard for beaches lacking bar-rip morphology. It is possible that the apparent decrease in hazard at RI 5 could be due to surfzone saturation under very large breakers causing shoreward bores that inhibit seaward rip flows (Castelle et al., 2016), especially at beaches lacking bar-rip morphology. However, the paucity of rip-related incidents under RI 5 at reflective and dissipative beaches is largely driven by the fact that H_b > 2.5 m occurred less frequently at those beaches than at intermediate beaches (Appendix C). This makes it difficult to achieve a statistically robust estimate of rip hazard at RI 5 for non-intermediate beaches but does not provide reliable evidence that hazard is reduced or absent.

Lifeguard-collected incident data has limitations, including poorly recorded or missing timestamps (impacting ability to link to forcing), subjective attribution to rip currents, subjective need for rescue to take place, and influence of water-user exposure and vulnerability on incident numbers. Where head count data are available to normalise incident numbers, they are not always reliable and are assumed to represent the average exposure over a given period. Furthermore, because of the unaccounted variation in water user vulnerability, the individual likelihood of an incident is a noisy proxy for hazard that is only useful when averaged over large numbers of incidents. Despite these limitations, the present analysis strongly supports conclusions from previous studies based on field experiments, numerical modelling, and lifeguard hazard perceptions that have found rip hazard increases during wave conditions at or above average breaker height with tide level at or below average low tide (Castelle et al., 2020; Moulton et al., 2017; Scott et al., 2014). This demonstrates that normalised incident numbers represent rip current hazard in a physically sensible manner. A unique strength of incident data is that it reveals conditions that most often lead to bathers getting into trouble due to rip currents. While this indirectly represents the physical hazard, it directly represents the outcome of most interest to coastal hazard managers.

Incident severity is often recorded by lifeguards. Incidents were not distinguished by severity in the present study as many non-environmental factors influence whether an incident is '*Life Threatening*' or even '*Fatal*' and filtering would have also

https://doi.org/10.5194/egusphere-2026-3638
Preprint. Discussion started: 8 July 2026

reduced the sample size considerably. However, previous studies of fatal rip incidents have demonstrated that low tide levels and average to above average wave height and period can be linked to the most severe rip incident outcomes (Castelle et al., 2020; Koon et al., 2023), supporting the rip index thresholds chosen in this study. Demographics were also not analysed here, but it is known that young males are over-represented in rip incident statistics (Castelle et al., 2018; Gensini and Ashley, 2010; Woodward et al., 2013), and in New Zealand over estimation of ability and underestimation of risk are thought to be contributing factors (Moran, 2011). Similar biases are expected in the present data set, and the incident likelihood statistics may over-represent young males compared to other demographic groups.

A degree of uncertainty is brought into the algorithm through the use of modelled tide and wave data (Albuquerque et al., 2021). This may explain, for example, why rip incidents were in some cases linked to very low energy conditions (Hs < 0.2 m, Tp < 5s) and may have been forced by larger waves in reality. Breaker conditions were estimated from nearshore model output locations using linear shoaling and Snell's refraction law (Larson et al., 2010), which leads to inaccuracies in locations that are sheltered within small embayments or where the nearshore morphology diverges significantly from a planar slope. At some forecast locations, this may lead to overprediction of hazard, as sheltering or wave dissipation through breaking may not be well represented. Beach morphology is a key driver for bathymetrically controlled rips and is accounted for in the present system only in a static, binary form, which assumes the presence or absence of bar-rip features is relatively static on a seasonal timeframe (Castelle et al., 2016; Scott et al., 2014). Dusek and Seim (2013) demonstrated some predictive skill by including a time-varying proxy for morphological relief in their algorithm, although it was found to have weaker predictive power than other variables (Dusek and Seim, 2013; Moulton et al., 2017). A generalisable and computationally inexpensive predictor for morphological relief of bar-rip features is yet to be demonstrated in the scientific literature but could help improve predictive skill in rip current forecasts.

The ability of the NZ rip forecast to achieve a high recall rate, capture increasing hazard at each Rip Index level, and conservatively agree with lifeguard hazard perceptions provides confidence that the system is appropriate for forecasting rip hazard in New Zealand. SLSNZ are now using this algorithm internally to forewarn lifeguard managers of times of peak rip hazard and are working on a technical and operational readiness plan to implement the rip hazard forecast publicly alongside water quality warnings on the 'Safeswim' online platform (https://safeswim.org.nz/). The former is expected to help mitigate rip current risk by informing lifeguard rostering days ahead of high-hazard times, while the latter could help remind water users of the risk posed by rips and help inform their decisions about where to bathe on a given day (for example, choosing a lifeguarded beach over a non-lifeguarded beach). Outside of New Zealand, the findings are potentially generalisable to other locations with comparable micro-meso tide range and associated beach morphology types, as the sampled wave conditions are common to most beaches globally (breaker heights and periods up to 4m and >15 s, respectively). The absolute thresholds in breaker height determined in the present are comparable to findings from other countries (Castelle et al., 2020; Dusek and Seim, 2013; Moulton et al., 2017; Scott et al., 2014). In particular, the 0.5 m and 1 m breaker heights we use to define thresholds at RI 2-3 align with the steep increase in rip likelihood observed in the USA by Dusek and Seim (2013). Comparable tide thresholds were also linked to increased rip incidents in the macrotidal setting of southwest UK (Scott et al., 2014, 2022), and

https://doi.org/10.5194/egusphere-2026-3638
Preprint. Discussion started: 8 July 2026

along the microtidal coast of Australia (Koon et al., 2023). With further testing, the New Zealand rip forecast may therefore provide a simple and computationally in-expensive means to forecast rips in other countries.

https://doi.org/10.5194/egusphere-2026-3638
Preprint. Discussion started: 8 July 2026

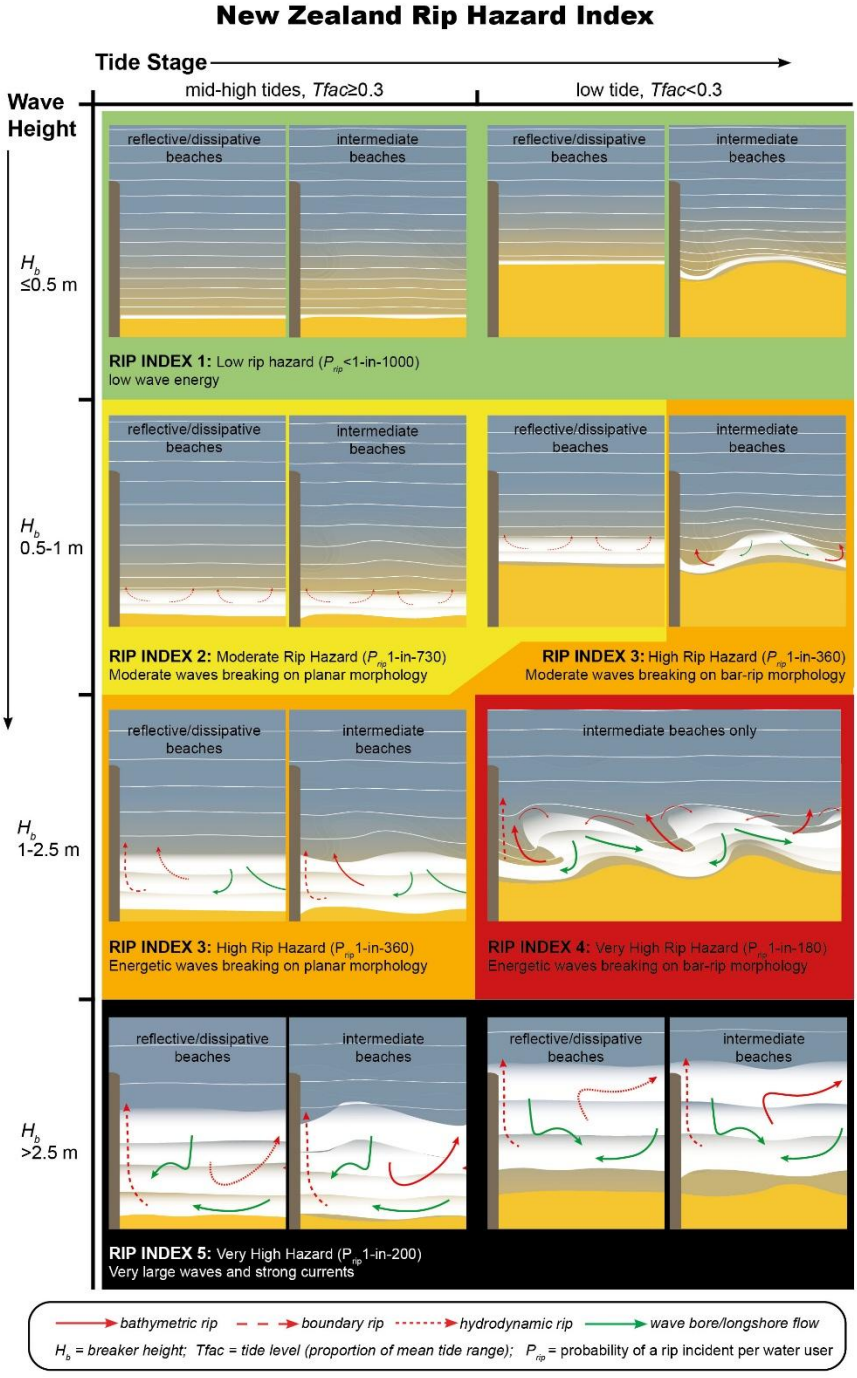

Figure 9. Diagram of the New Zealand Rip Hazard Index describing thresholds in H_b (significant breaking wave height) and $Tfac$ (tide level as a proportion of the average tide range), as well as conceptual rip behaviours and hazard level P_{rip} (incidents per water users exposed) associated with each Rip Index level.

https://doi.org/10.5194/egusphere-2026-3638
Preprint. Discussion started: 8 July 2026

5 Conclusions

This study utilised approximately 9000 rip incidents and associated lifeguard head counts spanning 21 years at 58 beaches in New Zealand to develop a threshold-based rip prediction algorithm. This was then compared to lifeguard hazard perceptions at 12 beaches over one summer season. To our knowledge, this represents the longest running rip incident data set analysed, and most widely validated rip forecast in the literature to date. The developed algorithm is extremely simple and uses no statistical modelling other than the identification of thresholds in key forcing variables known to contribute to rip hazard. The analysis shows strong agreement with previous findings from field experiments and numerical modelling in concluding that rip current hazard is disproportionately increased during wave conditions at or above average breaker height and with tide level at or below average low tide (Castelle et al., 2020; Moulton et al., 2017; Scott et al., 2014).

Rip currents were attributed to 53% of all SLSNZ recorded rescues made over the data record. Surprisingly, rip incidents were recorded under almost the full range of met-ocean conditions studied and no conditions (with the exception of zero wave energy) should be considered completely free of rip risk for water users. While bar-rip morphology was linked to the majority of rip incidents, they were also recorded by lifeguards at dissipative and reflective beaches in New Zealand. However, the data suggests that water users at intermediate beaches are 4 times more likely to be involved in a rip incident than those at dissipative beaches, and 25 times more likely than those at reflective beaches.

We have demonstrated using simple thresholds in breaker height and relative tide level, as well as consideration of beach morphology type, that high incident recall (2% false negatives) can be achieved with exponentially increasing rip hazard captured across five Rip Index levels. Because water user exposure has been accounted for, the developed Rip Index levels represent the physical hazard that is expected to occur, regardless of how many people enter the water. A water user is 6 times more likely to be involved in an incident at the highest Rip Index level (~1-in-200) than when Rip Index 1 is predicted (~1-in-1200), with warnings above Rip Index 3 given sparingly relative to the proportion of incidents they capture. The forecast algorithm captures past rip incidents best at beaches with intermediate ‘bar-rip’ morphology (99% recall) using thresholds based on breaker height and tide level, but acceptable skill is also achieved at reflective beaches (80% recall) and dissipative beaches (82% recall) using thresholds based on breaker height alone.

The predictions conservatively replicate lifeguard perceptions of rip hazard with an overall agreement rate (either exactly the same or one level higher) of 81%, providing confidence that the system can generate warnings consistent with those of a lifeguard. This provides opportunities to forewarn the public during times of high rip current hazard at un-lifeguarded beaches or outside lifeguard patrol hours. SLSNZ are now in the process of operationalising the NZ rip forecast algorithm nationally, on a public-facing web application. With further testing, the New Zealand rip forecast may provide a simple and computationally in-expensive means to forecast rips in other countries.

https://doi.org/10.5194/egusphere-2026-3638
Preprint. Discussion started: 8 July 2026

Code and data availability

Code and data may be partially available upon request. Surf Life Saving New Zealand lifeguard collected incident report forms can contain sensitive information relating to individuals. In some cases permission may also be required from local authorities to use these data.

Author contributions

All authors conceived of the presented idea and developed the theory. CS performed the data analysis for the beach classification, environmental forcing data, and lifeguard incident data. JAdM orchestrated and analysed the lifeguard perception data. AW, GM, and TS supervised the findings of this work. All authors discussed the results and contributed to the final manuscript.

Competing interests

The contact author has declared that none of the authors has any competing interests.

Acknowledgements

The authors are grateful to the many paid and volunteer lifeguards that diligently collected rip incident and head count data over the >20-year study period, as well as those who provided rip hazard perceptions for this research. The authors are also grateful to Giovanni Coco and Nelis Drost at the University of Auckland for providing the modelled wave and water level data at each beach location in the study.

Financial support

The research was funded by Surf Life Saving New Zealand. The pilot project was funded by Water Safety New Zealand and Auckland Council.

References

Aagaard, T., Greenwood, B., and Nielsen, J.: Mean currents and sediment transport in a rip channel, Mar. Geol., 140, 25–45, 1997.

Albuquerque, J., Antolínez, J. A. A., Gorman, R. M., Méndez, F. J., and Coco, G.: Seas and swells throughout New Zealand: A new partitioned hindcast, Ocean Model. (Oxf)., 168, 101897, 2021.

Arun Kumar, S. V. V and Prasad, K.: Rip current-related fatalities in India: a new predictive risk scale for forecasting rip currents, Natural hazards, 70, 313–335, 2014.

https://doi.org/10.5194/egusphere-2026-3638
Preprint. Discussion started: 8 July 2026

Austin, M., Scott, T., Brown, J., MacMahan, J., Masselink, G., and Russell, P.: Temporal observations of rip current circulation on a macrotidal beach, Cont. Shelf Res., 30, 1149–1165, 2010.

Austin, M. J., Scott, T. M., Russell, P. E., and Masselink, G.: Rip current prediction: Development, validation, and evaluation of an operational tool, J. Coast. Res., 29, 283–300, 2013.

Austin, M. J., Masselink, G., Scott, T. M., and Russell, P. E.: Water-level controls on macro-tidal rip currents, Cont. Shelf Res., 75, 28–40, 2014.

Brander, R. and Scott, T.: Science of the rip current hazard, in: The science of beach lifeguarding, CRC Press, 67–85, 2018.

Brander, R. W.: Field observations on the morphodynamic evolution of a low-energy rip current system, Mar. Geol., 157, 199–217, 1999.

Brander, R. W., Bradstreet, A., Sherker, S., and MacMahan, J.: Responses of swimmers caught in rip currents: Perspectives on mitigating the global rip current hazard, International Journal of Aquatic Research and Education, 5, 11, 2011.

Brighton, B., Sherker, S., Brander, R., Thompson, M., and Bradstreet, A.: Rip current related drowning deaths and rescues in Australia 2004–2011, Natural Hazards and Earth System Science, 13, 1069–1075, 2013.

Casper, A., Nuss, E. S., Baker, C. M., Moulton, M., and Dusek, G.: Assessing NOAA rip-current hazard likelihood predictions: comparison with lifeguard observations and parameterizations of Bathymetric and transient rip-current types, Weather Forecast., 39, 1045–1063, 2024.

Castelle, B., Bonneton, P., Senechal, N., Dupuis, H., Butel, R., and Michel, D.: Dynamics of wave-induced currents over an alongshore non-uniform multiple-barred sandy beach on the Aquitanian Coast, France, Cont. Shelf Res., 26, 113–131, 2006.

Castelle, B., Almar, R., Dorel, M., Lefebvre, J.-P., Senechal, N., Anthony, E. J., Laibi, R., Chuchla, R., and Penhoat, Y. du: Rip currents and circulation on a high-energy low-tide-terraced beach (Grand Popo, Benin, West Africa), J. Coast. Res., 633–638, 2014.

Castelle, B., Scott, T., Brander, R. W., and McCarroll, R. J.: Rip current types, circulation and hazard, Earth. Sci. Rev., 163, 1–21, 2016.

Castelle, B., Brander, R., Tellier, E., Simonnet, B., Scott, T., McCarroll, J., Campagne, J.-M., Cavailhes, T., and Lechevrel, P.: Surf zone hazards and injuries on beaches in SW France, Natural Hazards, 93, 1317–1335, 2018.

Castelle, B., Scott, T., Brander, R., McCarroll, J., Robinet, A., Tellier, E., De Korte, E., Simonnet, B., and Salmi, L.-R.: Environmental controls on surf zone injuries on high-energy beaches, Natural Hazards and Earth System Sciences, 19, 2183–2205, 2019.

Castelle, B., Scott, T., Brander, R., McCarroll, R. J., Tellier, E., de Korte, E., Tackuy, L., Robinet, A., Simonnet, B., and Salmi, L.-R.: Wave and tide controls on rip current activity and drowning incidents in Southwest France, J. Coast. Res., 95, 769–774, 2020.

Castelle, B., Dehez, J., Savy, J.-P., Liquet, S., and Carayon, D.: Physics-based forecast modelling of rip-current and shore-break wave hazards, Natural Hazards and Earth System Sciences Discussions, 2024, 1–30, 2024.

https://doi.org/10.5194/egusphere-2026-3638
Preprint. Discussion started: 8 July 2026

Castelle, B., Dehez, J., Savy, J.-P., Liquet, S., and Carayon, D.: Semi-empirical forecast modelling of rip-current and shore-break wave hazards, Natural Hazards and Earth System Sciences, 25, 2379–2397, 2025.

Churma, M. E., Kurkowski, N. P., Dusek, G., van der Westhuysen, A. J., Im, J.-S., Schattel, J. L., Alves, H., Padilla-Hernandez, R., Atkinson, D., and Chawla, A.: Observation methodologies for NOAA operational rip current forecast models, in: American Meteorological Society Meeting Abstracts, 2–3, 2017.

Coggins, J. H. J., Parsons, S., and Schiel, D.: An assessment of the ocean wave climate of New Zealand as represented in Kidson's synoptic types., International Journal of Climatology, 36, 2016.

Cornell, S., Peden, A. E., Brander, R., Roberts, A., Koon, W., and Lawes, J.: I actually thought that I was going to die: lessons on the rip current hazard from survivor experiences [conference abstract# 218], in: WCDP 2023 Shaping a global strategy. Mobilising for local action. Perth, Australia, December 5-7, 2023, 2023.

Costa, W., Bryan, K. R., Stephens, S. A., and Coco, G.: A regional analysis of tide-surge interactions during extreme water levels in complex coastal systems of Aotearoa New Zealand, Front. Mar. Sci., 10, 1170756, 2023.

Dusek, G. and Seim, H.: A probabilistic rip current forecast model, J. Coast. Res., 29, 909–925, 2013.

Engle, J., MacMahan, J., Thieke, R. J., Hanes, D. M., and Dean, R. G.: Formulation of a Rip Current Predictive Index Using Rescue Data, in: 2002 national conference on beach preservation technology, 1–14, 2002.

Gensini, V. A. and Ashley, W. S.: An examination of rip current fatalities in the United States, Natural Hazards, 54, 159–175, 2010.

Gibbs, A., Dusek, G., Van der Westhuysen, A., Santos, P., Huddleston, S., Estupiñan, J., Rivera, E., Stripling, S., and Padilla, R.: Numerical Validation of a Coupled Probabilistic Rip Current Model and Nearshore Wave Prediction System for South Florida, in: 95th AMS Annual Meeting/13th Symposium on Coastal Environment, 1–9, 2015.

Gorman, R. M., Bryan, K. R., and Laing, A. K.: Wave hindcast for the New Zealand region: nearshore validation and coastal wave climate, N. Z. J. Mar. Freshwater Res., 37, 567–588, 2003.

Hesp, P. A., Shepherd, M. J., and Parnell, K.: Coastal geomorphology in New Zealand, 1989-99, Prog. Phys. Geogr., 23, 501–524, 1999.

Kennedy, D. M., Sherker, S., Brighton, B., Weir, A., and Woodroffe, C. D.: Rocky coast hazards and public safety: Moving beyond the beach in coastal risk management, Ocean Coast. Manag., 82, 85–94, 2013.

Koon, W., Brander, R. W., Dusek, G., Castelle, B., and Lawes, J. C.: Relationships between the tide and fatal drowning at surf beaches in New South Wales, Australia: Implications for coastal safety management and practice, Ocean Coast. Manag., 238, 106584, 2023.

Larson, M., Hoan, L. X., and Hanson, H.: Direct formula to compute wave height and angle at incipient breaking, J. Waterw. Port Coast. Ocean Eng., 136, 119–122, 2010.

Lascody, R. L.: East central Florida rip current program, National Weather Digest, 22, 25–30, 1998.

Lee, J., Kim, I., and Lee, J. L.: Improving the Performance of Rip Current Forecasting Index with a Focus on Haeundae Beach, Korea, J. Coast. Res., 1556–1560, 2018.

https://doi.org/10.5194/egusphere-2026-3638
Preprint. Discussion started: 8 July 2026

Long, J. W. and Özkan-Haller, H. T.: Forcing and variability of nonstationary rip currents, J. Geophys. Res. Oceans, 121, 520–539, 2016.

Longuet-Higgins, M. S. and Stewart, R. W.: Radiation stresses in water waves; a physical discussion, with applications, in: Deep Sea Research and Oceanographic Abstracts, 529–562, 1964.

Lushine, J. B.: A study of rip current drownings and related weather factors, National weather digest, 16, 13–19, 1991.

MacMahan, J., Brown, J., Brown, J., Thornton, E., Reniers, A., Stanton, T., Henriquez, M., Gallagher, E., Morrison, J., and Austin, M. J.: Mean Lagrangian flow behavior on an open coast rip-channeled beach: A new perspective, Mar. Geol., 268, 1–15, 2010.

MacMahan, J. H., Thornton, E. B., Stanton, T. P., and Reniers, A. J. H. M.: RIPEX: Observations of a rip current system, Mar. Geol., 218, 113–134, 2005.

MacMahan, J. H., Thornton, E. B., and Reniers, A. J. H. M.: Rip current review, Coastal Engineering, 53, 191–208, 2006.

McCarroll, R. J., Brander, R. W., MacMahan, J. H., Turner, I. L., Reniers, A. J. H. M., Brown, J. A., Bradstreet, A., and Sherker, S.: Evaluation of swimmer-based rip current escape strategies, Natural Hazards, 71, 1821–1846, 2014.

McCarroll, R. J., Castelle, B., Brander, R. W., and Scott, T.: Modelling rip current flow and bather escape strategies across a transverse bar and rip channel morphology, Geomorphology, 246, 502–518, 2015.

Moran, K.: Perceived and real swimming competence among young adults in New Zealand, in: Proceedings of the World Drowning Prevention Conference, 202, 2011.

Moulton, M., Dusek, G., Elgar, S., and Raubenheimer, B.: Comparison of rip current hazard likelihood forecasts with observed rip current speeds, Weather Forecast., 32, 1659–1666, 2017.

Mouragues, A., Bonneton, P., Castelle, B., and Martins, K.: Headland rip modelling at a natural beach under high-energy wave conditions, J. Mar. Sci. Eng., 9, 1161, 2021.

Panofsky, H. W. and Brier, G. W.: Some Applications of Statistics to Meteorology, The Pennsylvania State University Press, Philadelphia, 1953.

Saulnier, D., Dixit, A., Nunes, A. R., and Murray, V.: Disaster Risk Factors–Hazards, exposure, and vulnerability, in: WHO Guidance on Research Methods for Health Emergency and Disaster Risk Management, World Health Organization, 151–163, 2020.

Scott, T., Austin, M., Masselink, G., and Russell, P.: Topographic Rip Currents Around Coastal Groyne Structures, Report produced for the Royal National Lifeboat Institute by the Coastal Processes Research Group (CPRG), Plymouth University, 44 pp., 2012.

Scott, T., Masselink, G., Austin, M. J., and Russell, P.: Controls on macrotidal rip current circulation and hazard, Geomorphology, 214, 198–215, 2014.

Scott, T., Masselink, G., Stokes, C., Poate, T., Wooler, A., and Instance, S.: A 15-year partnership between UK coastal scientists and the international beach lifeguard community, Cont. Shelf Res., 241, 104732, 2022.

Sickles, R. C. and Zelenyuk, V.: Measurement of productivity and efficiency, Cambridge University Press, 2019.

https://doi.org/10.5194/egusphere-2026-3638
Preprint. Discussion started: 8 July 2026

Sonu, C. J.: Field observation of nearshore circulation and meandering currents, J. Geophys. Res., 77, 3232–3247, 1972.

Stokes, C., Masselink, G., Revie, M., Scott, T., Purves, D., and Walters, T.: Application of multiple linear regression and Bayesian belief network approaches to model life risk to beach users in the UK, Ocean Coast. Manag., 139, 12–23, 2017.

Stokes, C., Poate, T., Masselink, G., Scott, T., and Instance, S.: New insights into combined surfzone, embayment, and estuarine bathing hazards, Natural Hazards and Earth System Sciences, 24, 4049–4074, 2024.

Walters, R. A., Goring, D. G., and Bell, R. G.: Ocean tides around new Zealand, N. Z. J. Mar. Freshwater Res., 35, 567–579, 2001.

Water Safety New Zealand: Coastal drowning deaths 2014-2024. Retrieved from DrownBase™ database, 2024.

Woodward, E., Beaumont, E., Russell, P., Wooler, A., and Macleod, R.: Analysis of rip current incidents and victim demographics in the UK, J. Coast. Res., 850–855, 2013.

Wright, L. D. and Short, A. D.: Morphodynamic variability of surf zones and beaches: A synthesis, Mar. Geol., 56, 93–118, 1984.

https://doi.org/10.5194/egusphere-2026-3638
Preprint. Discussion started: 8 July 2026

Appendix A. Surf life saving clubs contributing rip hazard perceptions and associated beach types

Table A1. List of Surf Lifesaving Clubs involved in collecting rip current hazard perceptions and their associated beach morphology classification (Section 0).

Surf Lifesaving club	Beach morphology type	Bar-rip morphology?
Lyall Bay SLSC	Low tide terrace	Yes
Maketu SLSC	Transverse bar and rip	Yes
Mt Maunganui LS	Low tide terrace	Yes
Omaha SLSC	Transverse bar and rip	Yes
Pacific SLSC	Reflective	No
Palmerston North SLSC	Rhythmic bar and beach	Yes
Papamoa SLSC	Transverse bar and rip	Yes
Riversdale SLSC	Transverse bar and rip	Yes
Taylors Mistake SLSC	Transverse bar and rip	Yes
Waihi Beach LS	Dissipative	No
Waipu Cove SLSC	Low tide terrace	Yes
Whiritoa LS	Transverse bar and rip	Yes

https://doi.org/10.5194/egusphere-2026-3638
Preprint. Discussion started: 8 July 2026

Appendix B. Rip Incident Reporting

The reporting in the incident records exhibits some inconsistencies, with a binary field for 'Rips/Holes' (Rip channels and associated rip flows are often referred to as 'holes' by SLSNZ lifeguards) present on the IRFs between 2001 – 2016, but no such field available for data between 2017 - 2022. Therefore, to arrive at the complete number of rip incidents mentioned above, a text search within the incident narratives was required to isolate any missing rip current incidents, especially for the period when a binary 'Rips/Holes' field was not used on the IRFs. Narratives including the words 'rip(s)' and 'current' were initially isolated and then manually verified, resulting in 1,170 additional rip incidents between 2017 - 2022. It is apparent from the number of recorded incidents per year (Fig. B1) that during the years when only free-text entries were used to describe the cause of incidents (2017-2022) far fewer rip incidents were recorded than in previous years. As there is no known reason for a statistical drop in incidents to have occurred, it is assumed that rip incidents were underreported during these years due to the need for free-text entry, or in some cases that incidents were missed by the text search because other terminology may have been used. It is therefore possible that the total proportion of incidents attributed to rip currents is even higher than the 53% stated above.

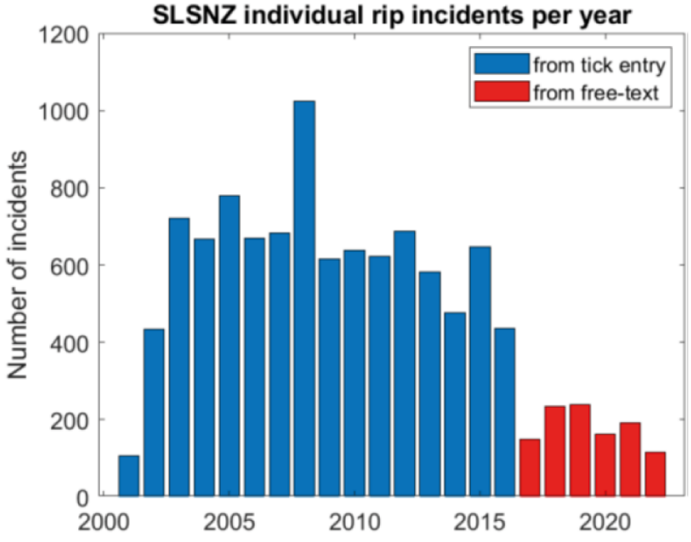

Figure B1. Number of rip current related incidents reported by SLSNZ lifeguards per year. Each incident represents one individual person rescued or assisted from a rip current.

https://doi.org/10.5194/egusphere-2026-3638
Preprint. Discussion started: 8 July 2026

Appendix C. Rip incidents and met-ocean conditions for different beach morphology types

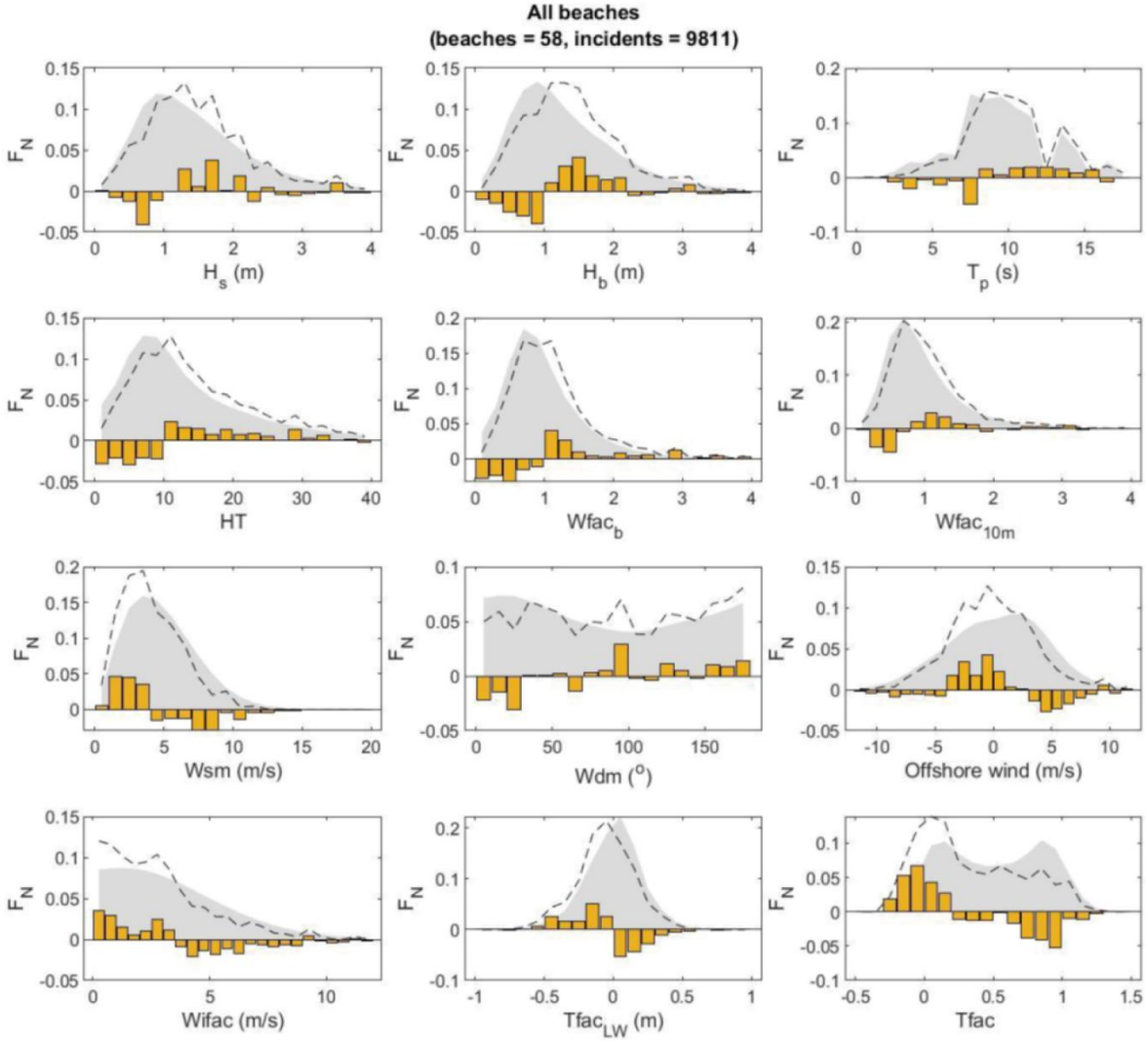

Figure C1. Normalised frequency distributions FN of key forcing variables at times of rip current incidents for all beaches studied. From L to R and top to bottom: significant wave height at 10 m depth (H_s) and at breaking (H_b), peak wave period (T_p), proxy wave power (HT), wave factor at break point ($Wfac_b$) and at 10 m water depth ($Wfac_{10m}$) both computed relative to Austral summer (Dec, Jan, Feb) mean, wind speed Wsm, wind direction relative to shore-normal Wdm, offshore directed wind component, cross-shore wind component Wifac, Tide Factor using the nearest low tide $Tfac_{LW}$, and Tide Factor using the instantaneous water level Tfac. Dashed lines show conditions occurring during rip current incidents, while grey shaded areas show the background distribution that occurs naturally over the Austral summer. The difference between the background and incident related distributions is shown as either a positive or negative orange bar, with positive (negative) bars indicating conditions associated with disproportionately more (less) rip current incidents.

https://doi.org/10.5194/egusphere-2026-3638
Preprint. Discussion started: 8 July 2026

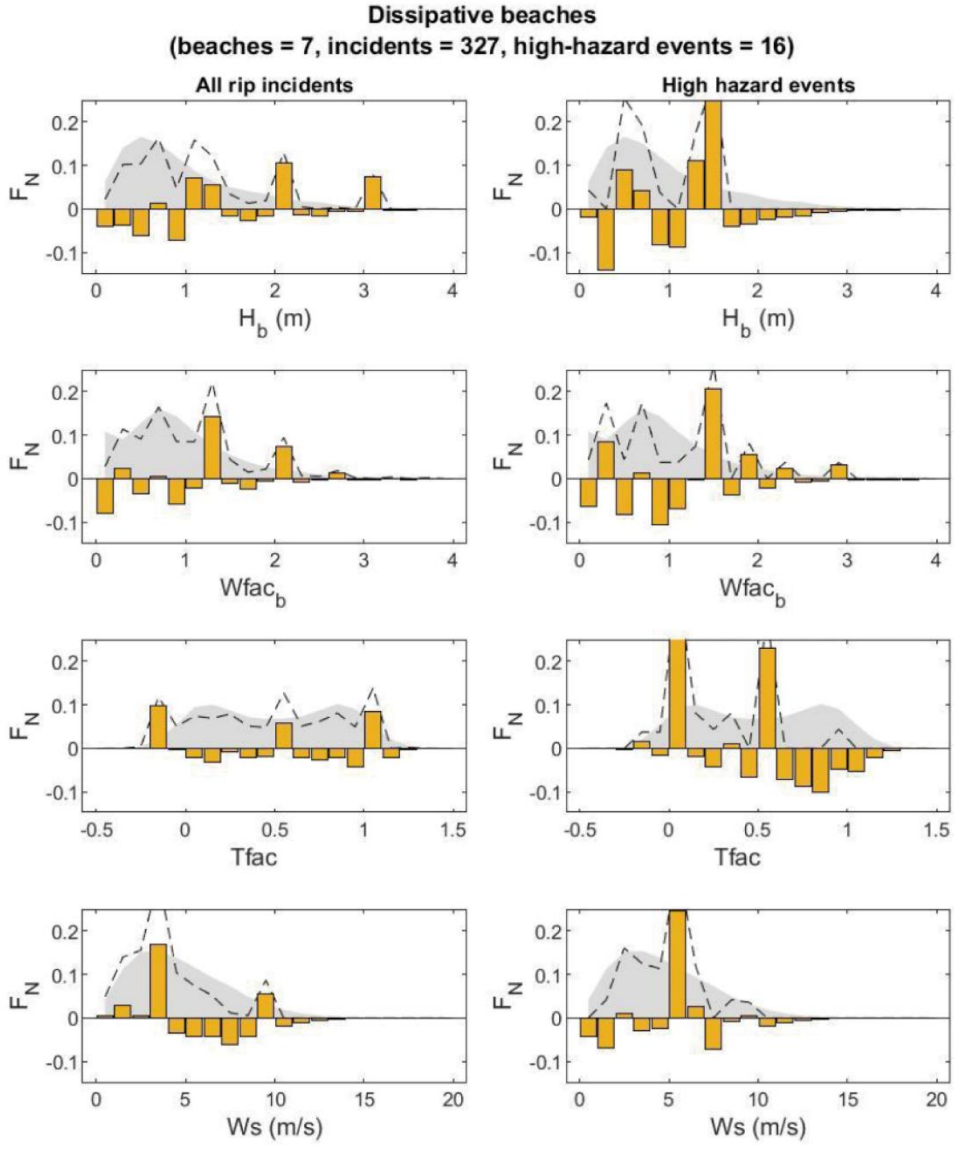

Figure C2. Normalised frequency distributions FN of key forcing variables at times of rip current incidents (left panels) and for P_{rip} > 90th%ile - 'high-hazard events' (right panels) at Dissipative beaches. From top to bottom panels show breaker significant wave height H_b, Wave Factor at break point $Wfac_b$, Tide Factor Tfac, and wind speed Ws. Dashed lines show conditions occurring during rip current incidents, while grey shaded areas show the background distribution that occurs naturally over the Austral summer (Dec, Jan, Feb). The difference between the background and incident related distributions is shown as either a positive or negative orange bar, with positive (negative) bars indicating conditions associated with disproportionately more (less) rip current incidents.

https://doi.org/10.5194/egusphere-2026-3638
Preprint. Discussion started: 8 July 2026

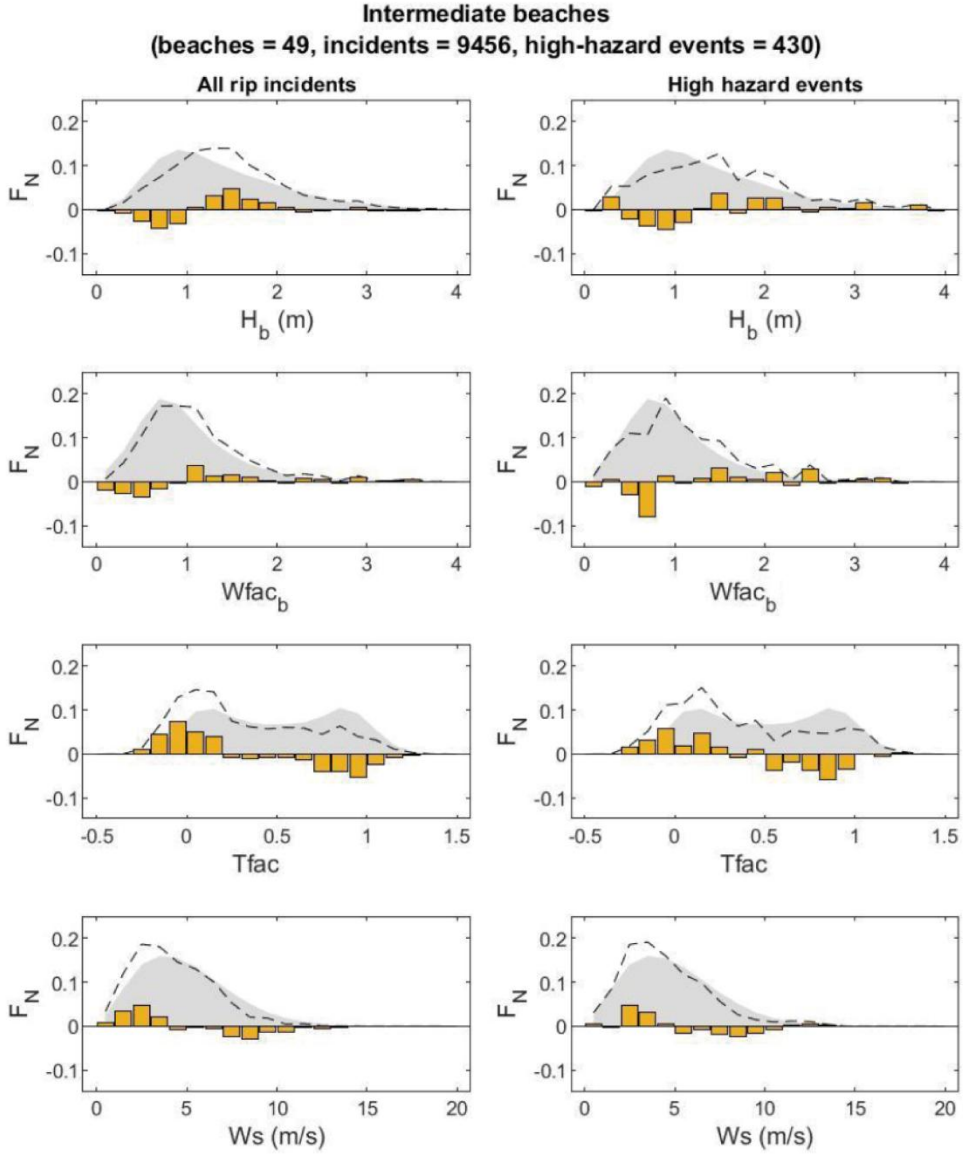

Figure C3. Normalised frequency distributions FN of key forcing variables at times of rip current incidents (left panels) and for P_{rip} > 90th%ile - 'high-hazard events' (right panels) at Intermediate beaches. From top to bottom panels show breaker significant wave height H_b, Wave Factor at break point $Wfac_b$, Tide Factor Tfac, and wind speed Ws. Dashed lines show conditions occurring during rip current incidents, while grey shaded areas show the background distribution that occurs naturally over the Austral summer (Dec, Jan, Feb). The difference between the background and incident related distributions is shown as either a positive or negative orange bar, with positive (negative) bars indicating conditions associated with disproportionately more (less) rip current incidents.

https://doi.org/10.5194/egusphere-2026-3638
Preprint. Discussion started: 8 July 2026

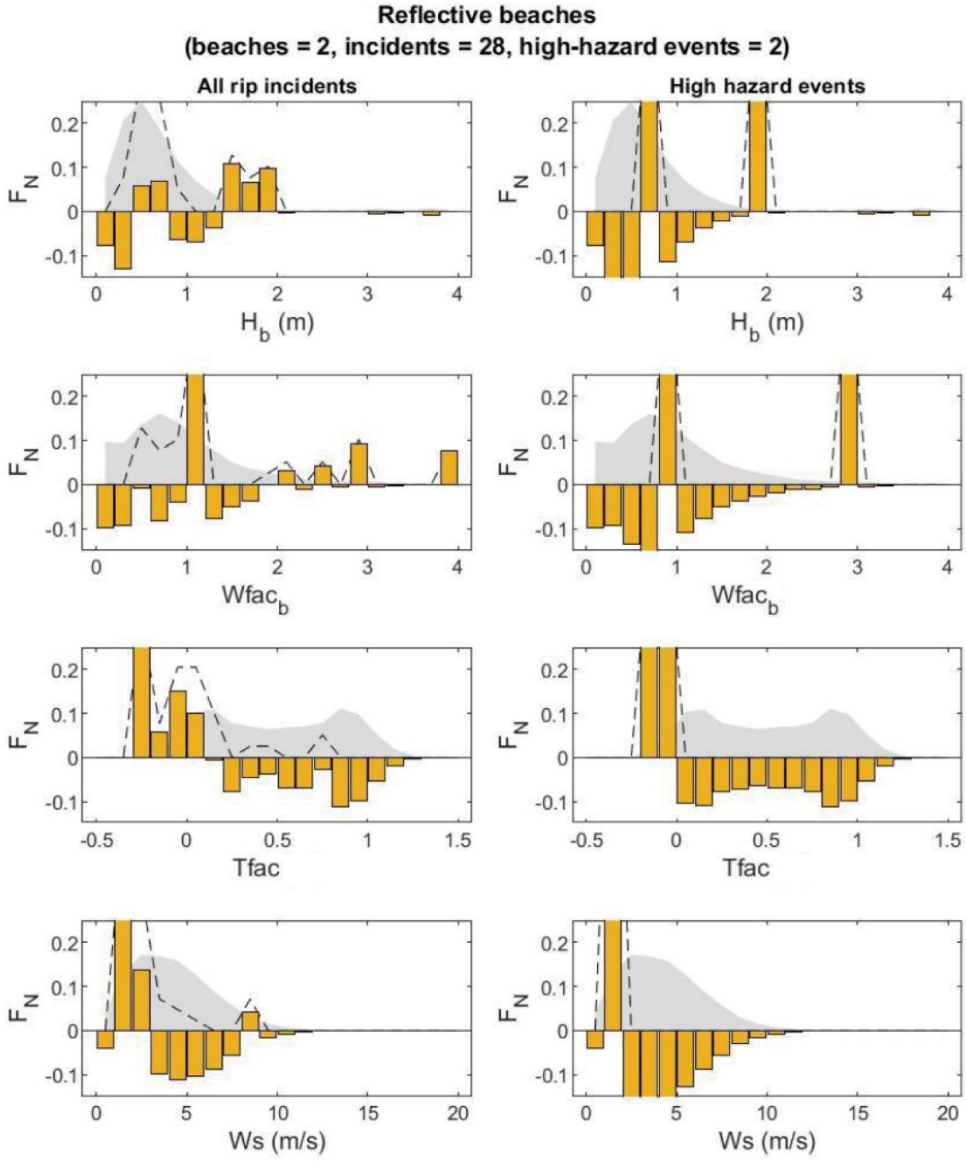

Figure C4. Normalised frequency distributions FN of key forcing variables at times of rip current incidents (left panels) and for P_{rip} > 90th%ile - 'high-hazard events' (right panels) at Reflective beaches. From top to bottom panels show breaker significant wave height H_b, Wave Factor at break point $Wfac_b$, Tide Factor Tfac, and wind speed Ws. Dashed lines show conditions occurring during rip current incidents, while grey shaded areas show the background distribution that occurs naturally over the Austral summer (Dec, Jan, Feb). The difference between the background and incident related distributions is shown as either a positive or negative orange bar, with positive (negative) bars indicating conditions associated with disproportionately more (less) rip current incidents.